Tackle environmental challenges in pollution controls using artificial intelligence: A review

Zhiping Ye[a], Jiaqian Yang[a], Na Zhong[a], Xin Tu[b], Jining Jia[c], Jiade Wang[a,*]

[a] College of Environment, Zhejiang University of Technology, Hangzhou 310014, PR China

[b] Department of Electrical Engineering and Electronics, University of Liverpool, Liverpool L69 3GJ, United Kingdom

[c] College of Chemical Engineering, Zhejiang University of Technology, Hangzhou 310014, PR China

*Corresponding author

E-mail address: jdwang@zjut.edu.cn.

Phone: +86-571-88320915. Fax: +86-571-88320882.

Abstract: This review presents the developments in artificial intelligence technologies for environmental pollution controls. A number of AI approaches, which start with the reliable mapping of nonlinear behavior between inputs and outputs in chemical and biological processes in terms of prediction models to the emerging optimization and control algorithms that study the pollutants removal processes and intelligent control systems, have been developed for environmental clean-ups. The characteristics, advantages and limitations of AI methods, including single and hybrid AI methods, were overviewed. Hybrid AI methods exhibited synergistic effects, but with computational heaviness. The up-to-date review summarizes i) Various artificial neural networks employed in wastewater degradation process for the prediction of removal efficiency of pollutants and the search of optimizing experimental conditions; ii) Evaluation of fuzzy logic used for intelligent control of aerobic stage of wastewater treatment process; iii) AI-aided soft-sensors for precisely on-line/off-line estimation of hard-to-measure parameters in wastewater treatment plants; iv) Single and hybrid AI methods applied to estimate pollutants concentrations and design monitoring and early-warning systems for both aquatic and atmospheric environments; v) AI modeling of short-term, mid-term and long-term solid waste generations, and various ANNs for solid waste recycling and reduction. Finally, the future challenges of AI-based models employed in the environmental fields are discussed and proposed.

Key words: Artificial neural network; Environmental pollutants; Intelligent control; Soft measurement; Early-warning

Contents

1. Introduction

One of the most remarkable progresses in the scientific community that has drawn almost all fields of researchers' attentions is the upsurge of artificial intelligence (AI). Since machine learning dominated mainstream researches in the 1990s, AI technology has rapidly developed and a plenty of AI methodologies are emerging and developing. AI technologies mainly refer to artificial neural network (ANN), support vector machine (SVM), genetic algorithm (GA), fuzzy logic (FL), etc., which have been applied to agriculture, climate, finance, engineering, security, education, medicine, nanotechnology and various disciplines (Chambers et al., 2018; Hong et al., 2018b; Lesnik and Liu, 2017; Nabavi-Pelesaraei et al., 2018; Offenberg et al., 2017; Pearce et al., 2013; Rocha et al., 2018; Wang et al., 2018; Zhang et al., 2017, 2019). Being considered as efficient and economical substitutes for conventional procedures and mathematics, these approaches are confirmed to provide a high level of capability for tackling the complexities of uncertain, interactive and dynamic problems.

The environmental pollutions are becoming the main concerns of the society, and the more stringent requirements and regulations for wastewater, air pollutants and solid waste treatment have stimulated the need for further improvement in this domain (Kannangara et al., 2018; Li and Zhu, 2018). However, most of the environmental pollution controls are associated with a number of factors with nonlinear, time-varying, multi-source and multi-objective characteristics, resulting in difficulties to achieve optimizing influential factors and desired system performance (Abiodun et al., 2018). At present, numerous studies have emphasized the applicability of statistical and multivariate data analysis methods on this subject, such as multiple linear regression (MLR) (Dieguez-Santana et al., 2016; Liu et al., 2019), response surface methodology (RSM) (Suárez-escobar et al., 2016; You et al., 2016), principal component analysis (PCA) (Tan et al., 2016), partial least squares regression (PLS) (Ferreira et al., 2017), k-means clustering algorithm (K-means) (C. Li et al., 2016), etc. The most widely discussed method is RSM, which is not included in the scope of machine learning algorithms. The results of studies that comparing these data analysis methods with AI models revealed that the former provides scientifically sounder information, together with statistical assessment and uncertainty estimations. However, AI technologies usually perform better in terms of accuracy in most works. For instance, Csábrági et

al. (2019) indicated that compared to MLR, the estimated DO in riverine ecosystems was closer to the actual experimental values. Fan et al. (2018) pointed out in their review that the GA-ANN and PSO-ANN models with the higher R^2 value and the smaller average error offered more accurate predictions than RSM for the removal efficiencies estimations of various pollutants. On the other hand, AI technologies are different from conventional mechanism modeling methods since they allow the omission of complex mathematical formulas and detailed information about the system that involves the relationships between the inputs and corresponding outputs without the loss of precision (Kalogirou, 2003). A large number of studies have indicated that AI technologies are good assistants for environmental pollution controls in wastewater (Fijani et al., 2019; Huang et al., 2015; Nag et al., 2018; Soleymani and Moradi, 2018; Yu et al., 2014, 2013), air pollution (He et al., 2017; Leng et al., 2017; Shang et al., 2019; Wang et al., 2018, 2017; Zhou et al., 2014) and solid waste (Abbasi and El Hanandeh, 2016; Adamovic et al., 2018; Fernández Núñez et al., 2017; Genuino et al., 2017; Selvakumar and Sivashanmugam, 2018). Meanwhile, it was reported some studies have also been carried out in climate change (Kashiwao et al., 2017; Zhang et al., 2019), natural water pollution (Bindal and Singh, 2019; Chang et al., 2014, 2015), and other environmental fields such as simulation of vegetation dynamics (Rocha et al., 2018; Ye et al., 2019) and early-warning of natural disasters (Bui et al., 2019; Jaafari et al., 2019; Kim et al., 2019) by using AI technologies. In view of AI widely used in environmental pollutants clean-ups, this paper will focus on the simulation, prediction, optimization and intelligent control of pollutant removal in the environments.

To the best of our knowledge, AI-aided applications in environmental clean-ups have been summarized in previous review publications, emphasizing on wastewater treatment processes, such as pollutants removal efficiency (Fan et al., 2018; Ghaedi and Vafaei, 2017; Khataee and Kasiri, 2010) and soft measurement (Haimi et al., 2013; Mohd Ali et al., 2015). As to the different kinds of AI techniques, the review papers mentioned above mainly focused on ANNs, resulting in a lack of comprehensive review on the applications of various AI-based technologies for environmental controls.

Hence, the objective of this review is to provide an up-to-date overview of AI technologies (e.g., ANN, SVM, FL, GA, etc.) in the processes of wastewater treatment, air pollution control and solid

117 waste treatment. Section 2 provides an overview of fundamental concepts of different AI methods,
118 and then introduces widely used single and hybrid AI methods. Next, the comprehensive
119 investigations of AI methods will be performed in the field of environmental controls, especially
120 intelligent control of wastewater treatment process, early-warning and assessment of air pollution,
121 and management of solid waste, all of which contributes novel and important aspects in this
122 review. At last, future challenges of AI methods will be discussed.
123

2. Categories and fundamentals of AI methods for environmental pollution controls

In general, AI modelings are implemented using software tools (i.e., MATLAB (Barzegar et al., 2018; Sabour and Amiri, 2017; Shokry et al., 2018) and NeuroSolutions (Nag et al., 2018)) that support C/C++ Language, Java, Python, or other programming languages. Among these software, MATLAB is the most accepted software since its ready-to-use toolboxes are quite convenient and applicable for beginners that are not directly working in AI field, like environmental researchers. A classification tree of AI technologies widely used in environmental field can be seen in Fig. 1. Among all of these methods, ANNs are found to be the mainstream AI technologies. It was reported that most researchers use a single ANN model or a hybrid model including ANN (e.g., fuzzy neural network (FNN) and adaptive network-based fuzzy inference system (ANFIS)) due to easy implement with relative high accuracy. The characteristics and comparisons of the popular single and hybrid AI methods in this field are given in Table 1. Detailed discussions will be presented in following chapters.

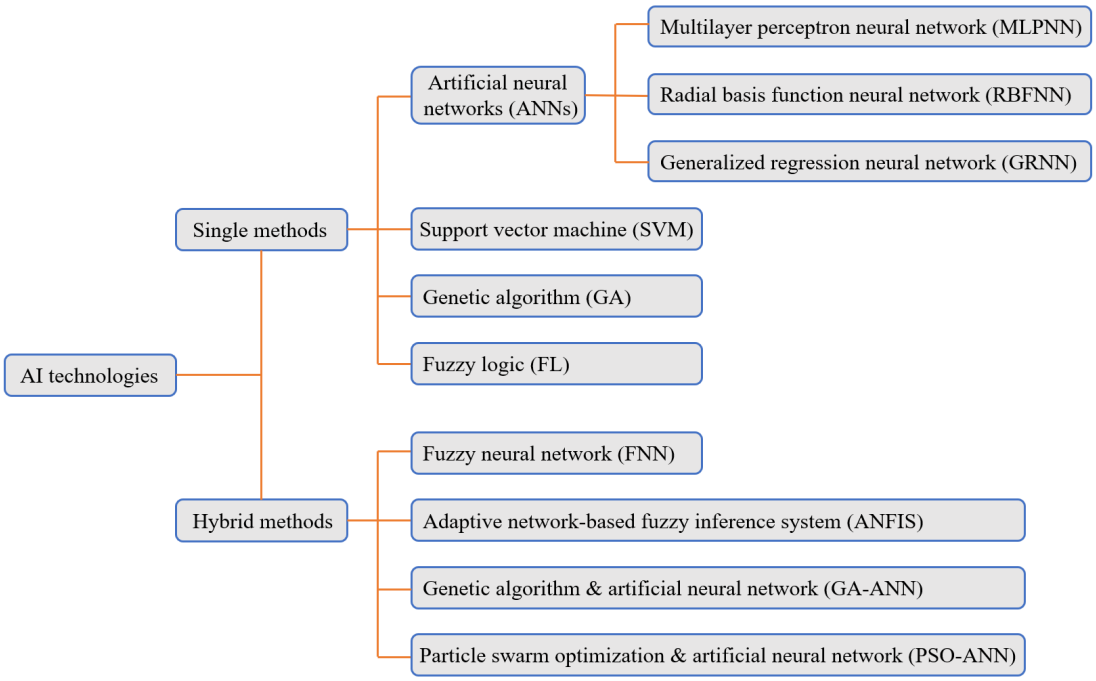

Fig. 1. A classification tree of AI technologies for environmental pollution controls.

141 **Table 1** Characteristics and comparison of the mainstream AI technologies used for environmental pollution controls.

No.	Types of AI technologies	Characteristics	Advantages	Limitations
1	Multilayer perceptron neural network (MLPNN)	● Supervised learning ● Back-propagation algorithm is widely used as training algorithm	● Easy to implement ● High accuracy and consistent estimations when changes occur	● Slow speed of convergence ● Numbers of hidden neurons always based on trial and error ● Risks of over-fitting and local minimum
2	Radial basis function neural network (RBFNN)	● Basis function used can be Gaussian or wavelets ● Universal approximation	● High tolerance of noise ● Fast training ● Good capability in generalization	● Require large amount of training data ● Large number of hidden neurons needed
3	Support vector machine (SVM)	● Based on the structured risk minimization principle ● Use quadratic programming to solve support vector	● Small data required ● Global searching ability ● High robustness against noise	● Large memory requirement and CPU time when trained in batch mode
4	Genetic algorithm (GA)	● Simulates natural selection and genetic mechanisms of biological evolutionary theory ● Universal approximation ● Heuristic algorithm	● Good global optimization capability ● Generate feasible solutions and allow researchers to choose from several approaches for obtaining best results ● Flexibility to combine with other methods or models	● Several trial and errors before reaching the ideal new generations ● Computational heaviness
5	Fuzzy neural network (FNN)	● Contain theory of fuzzy logic and ANN ● Human-like reasoning ● Suitable for advanced control systems	● If-then rules easy to interpret ● Implementation can be either from input to output or output to input ● Able to accurately describe imprecise values of parameters	● Challenges in choosing network topology ● Long computational time ● Low robustness against noisy data
6	Adaptive network-based	● Consist of antecedent and conclusion	● Efficient nonlinear approximation	● Optimum structures are based on trial

	fuzzy inference system (ANFIS)	● Integrate gradient descent method and least square method to train parameters	● Short learning time ● Fast in reaching optimum results	and error
7	Artificial neural network coupled with genetic algorithm (GA-ANN)	● Weights and thresholds of neural network are optimized by GA ● Predicted output value of neural network can be used as the fitness function of GA.	● Prevent local minimum ● Fast convergence ● High accuracy	● Computational heaviness ● Unable to determine numbers of hidden neurons

142

143

2.1 Artificial neural networks (ANNs)

ANNs are being broadly employed as approaches for prediction, classification and optimization in various fields due to their remarkable capacity to capture the nonlinear behavior between independent and dependent variables based on historical data using an applicable training algorithm (Ghaedi and Vafaei, 2017; F. J. Li et al., 2016). There are several different classifications of ANNs, this chapter focuses on the typical types of configurations that have been employed in research works of environmental controls, such as feedforward neural networks, specifically multilayer perceptron networks (MLPNN) and radial basis function neural network (RBFNN).

2.1.1 Multilayer perceptron neural network (MLPNN)

MLPNN is one of the simplest and the most well-known type of ANNs. The structure of MLPNN, which includes input layer, hidden layer and output layer, has a significant impact on predictive capability. Independent and dependent parameters determine the numbers of neurons in the input and output layer, respectively. Neurons numbers in the hidden layer are generally determined via the procedure using the trial and error observation, rather than being specified at first (Zonouz et al., 2016). Insufficient hidden layer neurons make the network difficult to fully learn the data laws, causing under-fitting problems. However, excessive neurons may lead to over-fitting as a result of extra degrees of freedom. Normally, MLPNN model begins with fewer neurons in the hidden layer, and then the numbers of neurons will be updated in the training process by adjusting the numbers of neurons, so far there aren't any systematic methods to define the optimal numbers of neurons in hidden layer (Bahrami et al., 2017; Moosavi and Soltani, 2013). Based on specific neurons and weights contained in each layer, as well as an appropriate training algorithm, a well-trained MLPNN is capable of generating principle to track nonlinear input-output relationships, giving predicted values of the corresponding output(s) based on input conditions (Ghaedi and Vafaei, 2017).

A MLPNN trained by back-propagation (BP) algorithms, also known as the back-propagation neural network (BP-ANN), is the most representative type of ANN which is widely applied in the field of environmental pollution controls. Fig. 2 shows that the input signals are processed through

the hidden layers, and the output signals are generated through nonlinear transformation. The state of neurons in each layer only affects the neurons in the next layer. The correlation between the input x_i and output y_j from a neuron in the hidden layer can be expressed as follows:

$$y_j = f\left(\sum_{i=1}^{n} w_{ij}x_i + b\right) \quad (1)$$

where y_j is the jth output in the hidden layer, $f(x)$ is the transfer function, n is the number of input variables, w_{ij} denotes the weight from element i in input layer to element j in the hidden layer, x_i is the ith output from the input layer, and b is the bias of hidden layer. The signals generated from the output neuron are the conversion of the weighted sum of output signals in the hidden layer.

Standard BP is based on a gradient search, in which the network weights and thresholds move backwards along the performance function gradient, minimizing the errors between the actual output values of the network and the expected output values (Wang et al., 2018). The learning algorithm employed for weights correction can be expressed as follows:

$$\Delta w_{ij}(s+1) = -\eta \frac{\partial E}{\partial w_{ij}} + \mu \Delta w_{ij}(s) \quad (2)$$

where $\Delta w_{ij}(s)$ is expressed as the correction of the weight at the sth learning step, η denotes the training rate, E denotes the total sum squared error of all data in the training set, μ is the momentum factor.

The weights and thresholds of all the neurons are being updated until all the errors are located within the required tolerance or the maximum number of iterations is achieved (Fan et al., 2018; Kalogirou, 2003; Khataee and Kasiri, 2010). Fig. 2 illustrates the process of information conversion in a single neuron (A) and a typical MLPNN with two hidden layers (B).

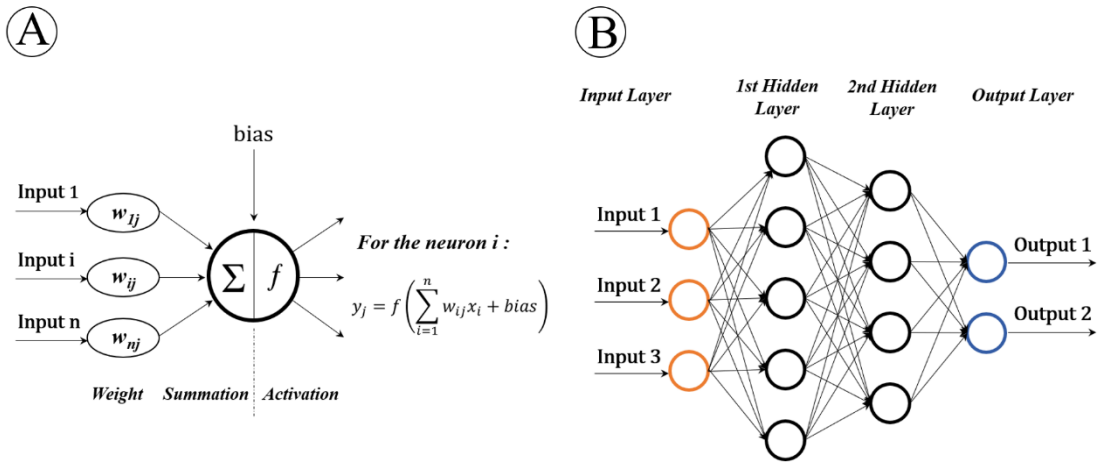

Fig. 2. Information processing in a neuron (A) and typical MLPNN architecture (B).

Early studies have indicated that a single-hidden-layer network with a sufficient number of neurons in its hidden layer can approximate any input-output relationship to a desired accuracy (Despagne and Massart, 1998; Lek and Guegan, 1999). Single-hidden-layer MLPNN coupled with BP learning algorithm is found to be the most widely used type of ANN. More fundamentals of the MLPNN can be found elsewhere (Kalogirou, 2003; McCulloch and Pitts, 1943), and details about the principles in exploiting an ANN can be found in Ghaedi and Vafaei (2017), Kalogirou (2003), and Khataee and Kasiri (2010).

2.1.2 Radial basis function neural network (RBFNN)

RBFNN is another type of neural network, which relies on radial basis functions (RBF) as activation functions (Nandagopal et al., 2017; Turan et al., 2011). Comparing to MLPNN, RBFNN is identified as a superior ANN model due to its ability to map principles with a high tolerance of input noises and online learning, even though more data are required to obtain more reliable results (Buyukyildiz and Kumcu, 2017; Zhu et al., 2017). On the one hand, an RBFNN is one of the feedforward neural networks based on supervised learning similarly to MLPNN. On the other hand, it is also a weighted linear combination of RBF, which typically includes three different layers, i.e. input layer, Gaussian RBF layer, and linear output layer, differing from MLPNN in internal calculation structure (Singh et al., 2013; Tatar et al., 2016). Gaussian transfer function, which is employed in the neurons of hidden layer (RBF units), generates inversely proportional outputs to the expanse from the center of the neuron. Each unit is characterized by the location of the function's center C_k and its bandwidth σ_k, both of which are critical to model accuracy and

generalization abilities (Zhu et al., 2017). As shown in Fig. 3, a single-output RBFNN with a hidden layer with M neurons is defined as

$$y(t) = \sum_{k=1}^{M} W_k \theta_k(x(t)) \tag{3}$$

Where x and y stand for the input and output of the network, respectively, W_k is the connecting weights between the kth hidden neuron and the output neuron, $\theta_k(x)$ is the output value function of the kth hidden neuron, which is defined as follows:

$$\theta_k(x(t)) = exp\left(-\frac{\|x(t) - \mu_k(t)\|}{\sigma_k^2}\right) \tag{4}$$

Where μ_k represents the center vector of the kth hidden neuron, σ_k^2 denotes the radius or width of the kth hidden neuron, and $\|x - \mu_k\|$ stands for the Euclidean distance between x and μ_k.

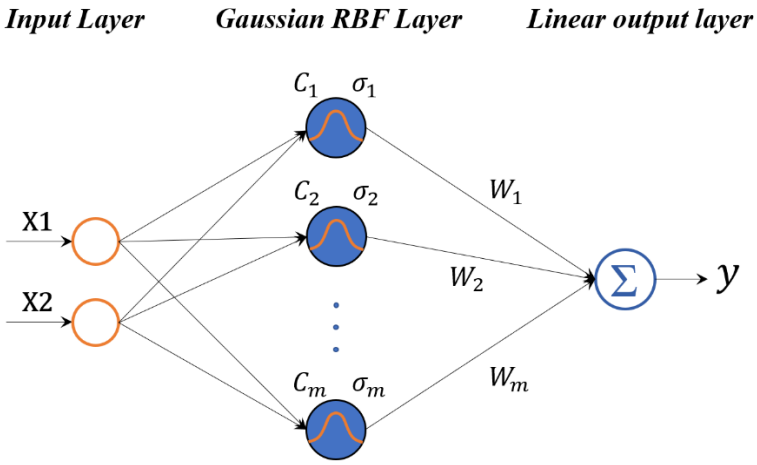

Fig. 3. Structure of RBFNN with a single output.

Conventionally, some random data points are chosen as the RBF center, and singular value decomposition (SVD) method is employed for network training. Due to the unsteadiness of RBFNN conducted by the basic algorithms above, improved algorithms such as k-means clustering algorithm and orthogonal least square algorithm (OLS) are recently used to select center points of RBF (Turan et al., 2011). Moreover, the number of hidden layer neurons is another parameter that needs to be determined before developing a network. Updated RBFNN have been employed to settle this problem, for example, flexible structure radial basis function neural network (FS-RBFNN) in which the hidden neurons can be removed or added online relying on the

neuron activities and mutual information (Han et al., 2011). More details of the RBFNN can be found elsewhere (Chien-Cheng et al., 1999; Park and Sandberg, 1991).

It was reported that general regression neural network (GRNN) as a special variation of the RBFNN had been used in the field of environmental pollution controls (Adamovic et al., 2018; Antanasijevic et al., 2013; Huang and Chen, 2015; Singh et al., 2012; Zhou et al., 2014). Based on nonlinear Gaussian kernel regression, a GRNN has strong nonlinear mapping ability and is able to obtain reliable results even when the data is unstable. It is notable that GRNN can estimate any random function between the input and output variables, displaying the function estimate directly from the training data without any iterative training procedure (Buyukyildiz and Kumcu, 2017; Singh et al., 2013).

2.2 Support vector machine (SVM)

As a new machine learning technology introduced firstly by Vapnik (1995), SVM is developed to minimize the upper bound of generalization error based on the structured risk minimization principle (Pai et al., 2010; Vapnik, 1995). SVM is able to achieve good generalization results in both classification and regression, because the convergence principle gives it greater ability to regress the relationship of input and output values and to obtain satisfactory performance for new input data (Chen, 2011; Jaramillo et al., 2018).

Recently, support vector regression (SVR), known as a regression version of SVM, is considered as an efficient alternative technology to tackle regression problems in the field of the environmental controls by introducing a selective loss function. The main idea of SVR can be defined as following equation:

$$f(x) = \sum_{i=1}^{M} W_i \phi(x_i) + b \tag{5}$$

where x and $f(x)$ denote the input and output values of SVR, respectively, M is the total number of data patterns, $\phi(x_i)$ denotes the space with high-dimensional feature, which can be nonlinearly mapped from the input space, and the coefficients W_i and b are calculated by the means of minimizing regularized risk function as follow:

$$R_{SVR}(C) = R_{emp} + \frac{1}{2}\|W\|^2 = C \times \frac{1}{N}\sum_{i=1}^{N} L_\varepsilon(d_i, y_i) + \frac{1}{2}\|W\|^2 \quad (6)$$

$$L_\varepsilon(d_i, y_i) = \begin{cases} |d_i - y_i| - \varepsilon, & 0 \\ |d_i - y_i| \geq \varepsilon, & \text{otherwise} \end{cases} \quad (7)$$

where R_{SVR} and R_{emp} denote the regression and empirical risks, respectively, the term $\|W\|^2 / 2$ is employed as a measurement of function flatness, C represents a cost function measuring the empirical risk, ε represents insensitive error constant, and the term $L_\varepsilon(d_i, y_i)$ denote an ε-insensitive loss function for empirical error estimation. When an error occurs, the regularized constant C will be used to calculate the penalty by controlling the trade-off between the empirical risk and the regularization term. On the other side, the ε-insensitive loss function is utilized to minimize the noise and stabilize estimation, making ε another essential parameters that should be considered comprehensively in the empirical analysis (Chen, 2011; Leng et al., 2017; Wang et al., 2015).

The theory of least squares-support vector machine (LS-SVM) is introduced based on the traditional SVM. LS-SVM has currently emerged as an attractive semi-supervised statistical learning technology, which is applied to solve the problems of multivariate calibration rapidly (Asfaram et al., 2016a; Ghaedi et al., 2014; Mahmoodi et al., 2016). The least squares linear system can assist SVM to sovle the regression and classification problems comparing to traditional SVM with direct quadratic programming. Besides, it is easier to develop LS-SVM models because only two variables, namely the kernel parameter (σ2) and the regularization parameter (γ), were required to obtain desired results (Ghaedi and Vafaei, 2017). More basic information on SVM and LS-SVM were detailed discussed in Scholkopf and Smola (2001), Suykens and Vandewalle (1999), Vapnik (1995), and Zhao (2015).

2.3 Heuristic algorithms

The evaluation index, such as root mean square error (RMSE) and coefficient of determination (R^2), indicate that single AI method could achieve satisfactory performance in some cases, while it is revealed that single AI models coupled with heuristic algorithms could achieve faster convergence, better global search capability and better generalization performance. More specifically, various heuristic algorithms can be employed to obtain the initial weights and

thresholds of ANNs, to define the center of the RBF function, and also to obviate the risk of being trapped at shallow local optima.

Inspired by natural phenomenon or social behavior, heuristic algorithms (such as genetic algorithm (GA), particle swarm optimization (PSO), immune algorithm (IA), artificial bee colony (ABC), etc.) were revealed to be suitable replacements for the traditional algorithms (e.g. BP algorithm) to obtain the global optimum solution in a quick and efficient way (Arhami et al., 2013; Biglarijoo et al., 2017; Hong et al., 2018a; Oliveira et al., 2019; Yilmaz et al., 2018). As the two most popular heuristic algorithms in environmental field, GA and PSO would be discussed.

GA, a stochastic general search technology enlightened by the biological evolution principles in the natural genetic system, has been employed to solve optimization problems (Al-Obaidi et al., 2017; Hoseinian et al., 2017). The general optimization strategy underlying the method will generate a population of represented random solutions, and then genetic operators, such as selection, crossover and mutation, will be applied for the generation of a new and better population. Every single solution is evaluated by a fitness function, and the whole process will repeat until convergence is obtained (Oliveira et al., 2019; Yasin et al., 2014). More details of the GA can be found elsewhere (Davis, 1991; Goldberg and Holland, 1988). Generally, GA is embedded in an ANN to update the initial weights, thresholds in hidden and output layers to overcome the local minima problem. It seems that the GA-ANN is prospective method for design and selection of the heterogeneous catalytic materials, which are used in treatment of wastewater and air pollution, and the production of clean energy (Bahrami et al., 2017; Hadi et al., 2016; Izadkhah et al., 2012; Niaei et al., 2013; Zonouz et al., 2016). Recent research works also suggested that GA is able to generate fuzzy rules and optimize membership functions of fuzzy sets. The combination of GA, ANN, and fuzzy logic (FL) was proved to be a powerful approach for integrated process modeling and optimization, particularly for some multi-objective optimization control problems (Huang et al., 2015; Strnad and Guid, 2010).

PSO as another widely used evolutionary computation method is enlightened by the foraging behavior of a bird flock. This strategy has been well recognized as an efficient technique for results optimization and intelligent search (Fan et al., 2017; Xu and Yu, 2018). The initial population of PSO is generated randomly with positions and velocities, and each particle

316 represents a potential solution of the optimization problem. Then every single particle will be
317 evaluated by a fitness function, a new position with better fitness value will be selected, and the
318 position of particles will be updated continually by moving toward maximum objective function.
319 Eventually, an optimal solution is obtained when the number of iterations reaches the maximum
320 (Agarwal et al., 2016; Khajeh et al., 2017, 2013). The further information of PSO can be found
321 elsewhere (Eberhart and Yuhui, 2001; Shi and Eberhart, 1998).

322 Both of GA and PSO use fitness function to evaluate solutions, and both perform random
323 searches based on fitness values, but PSO depends on the particle velocity for the completion of
324 search process with higher convergence rate comparing to GA. On the other hand, PSO lacks the
325 dynamic velocity adjustment resulting in easier to get trapped into local optima, this would cause
326 convergence difficulties and low convergence accuracy. In all, it seems more feaible to use GA in
327 research of environmental fields due to good global search capability.

328 **2.4 Hybrid intelligent systems**

329 Hybrid intelligent systems (e.g. ANFIS, FNN, GA-ANN, etc.) are systems which combine two
330 or more AI technologies to overcome certain shortcomings in a single AI method, achieving
331 synergistic advantages. For most complicated nonlinear problems, AI methods have many
332 advantages over traditional methods. However, each AI method has its limitations (as seen in
333 Table 1), causing the difficulty to achieve the expected results. Give an example, a three-layer
334 MLPNN has strong nonlinear mapping abilities and can approximate any nonlinear continuous
335 functions. However, the convergence rate of MLPNN is slow, and there is a risk of overfitting and
336 local minimum. Taking advantage of two or more AI technologies to construct a hybrid system is
337 an effective way to solve such problems. For instance, SVM can achieve global optimization and
338 eliminate overfitting in the ANN framework (Taghvaei et al., 2016), GA and PSO have been
339 widely applied to optimize the initial thresholds and weights of ANN for improving its reliability
340 and generalization performance (Hoseinian et al., 2017).

341 The classical hybrid system is the neuro-fuzzy system, other types of hybrid system, such as
342 heuristic algorithms coupled with different types of ANNs, SVM models or fuzzy systems, are
343 considered to be efficient tools to solve complicate problems. Since neuro-fuzzy system is widely
344 used as a optimization tool in treatment of wastewater field, more details will be discussed.

Among the neuro-fuzzy systems, adaptive network-based fuzzy inference system (ANFIS) is proved to be a powerful tool in many fields, such as forecasting, controlling, data mining and noise elimination (Bagheri et al., 2017; Hong et al., 2018a; Huang et al., 2009; Pai et al., 2011; Wan et al., 2011). Based on Takagi-Sugeno fuzzy inference system, an ANFIS is a feedforward neural network coupled with FL to illustrate nonlinear behavior in complicate systems, in other words, a fuzzy inference system (FIS) employed in the configuration of adaptive neural networks (Huang et al., 2009). As shown in Fig. 4, the framework of an ANFIS model contains the antecedent and the conclusion, that are connected by fuzzy rules in the form of networks. Since ANFIS integrates the learning capacities of the neural network and reasoning abilities of the fuzzy system, synergistic advantages can be achieved in one hybird model (Huang et al., 2015; Mohd Ali et al., 2015). More details of the ANFIS can be found in other literatures (Jang, 1993; Yilmaz and Kaynar, 2011).

Hybrid technologies that combine machine learning algorithms with statistical and multivariate data analysis methods are currently emerging. For instance, principal component analysis (PCA) was employed to extract variables with high contribution rates from the initial dataset. Experimental design methods such as orthogonal experimental design and response surface methodology (RSM) have been used to obtain representative experimental data. These hybrid technologies make supervised learning more flexible, and improve the accuracy of AI models to some extent (Gadekar and Ahammed, 2019; Xie et al., 2018).

It's worth noting that hybrid AI systems can't be employed to all circumstances. The higher integrated the approach, the more complex the model structure. Hence, it will be more difficult for hybrid AI systems development. In this regard, hybrid methods are not preferred when a single AI method is sufficient to describe the input-output relationships with satisfactory results. Further information on hybrid intelligent systems can be found in Goonatilake and Khebbal (1994) and Medsker (1995).

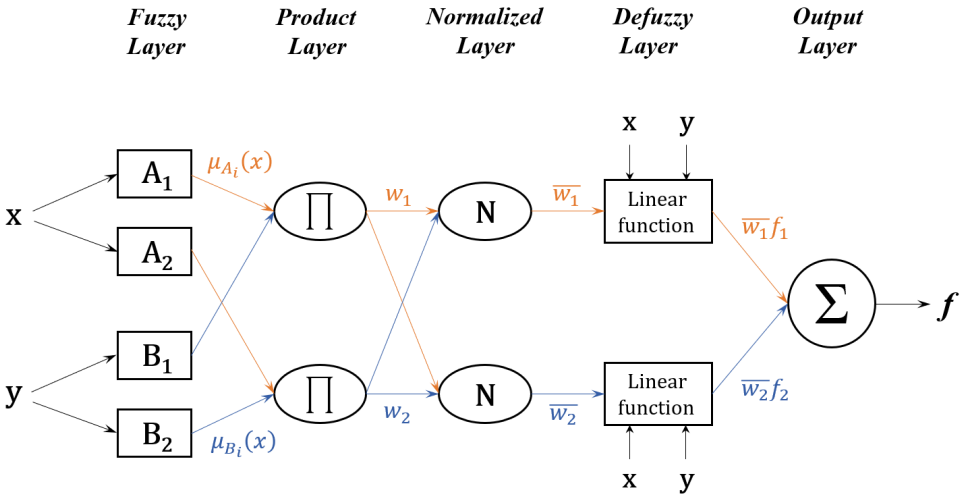

Fig. 4. Configuration of typical ANFIS.

3. AI technologies for environmental controls

To the best of our knowledge, AI technologies have been employed extensively in dealing with wastewater, air pollution as well as solid waste, playing a leading role in modeling, optimization, prediction and control. The evolution over the time of the numbers of publications is presented in Fig. 5. Obviously, many studies related to environmental controls are rapidly increasing in the past decade. Modeling complex environmental problems using AI technologies is becoming popular in environmental field, especially in wastewater treatment.

The model performance is evaluated using statistical parameters, mainly involving the R^2 and RMSE. The R^2 indicates the degree of correlation between the experimental and predictive values, which can be expressed as the equation below:

$$R^2 = 1 - \sum_{i=1}^{N} (y_p - y_e)^2 \Big/ \sum_{i=1}^{N} (y_p - \bar{y_e})^2 \quad (8)$$

where N is the number of model output, y_p is the predictive output value, y_e stands for the experimental value, and $\bar{y_e}$ denote the average values of the experiments. The RMSE indicates the errors between the experimental values and model outputs as following equation shown:

$$\mathrm{RMSE} = \sqrt{\frac{1}{N} \sum_{i=1}^{N} (y_p - y_e)^2} \quad (9)$$

Here, higher value of R^2 and lower value of RMSE indicate a better prediction performance.

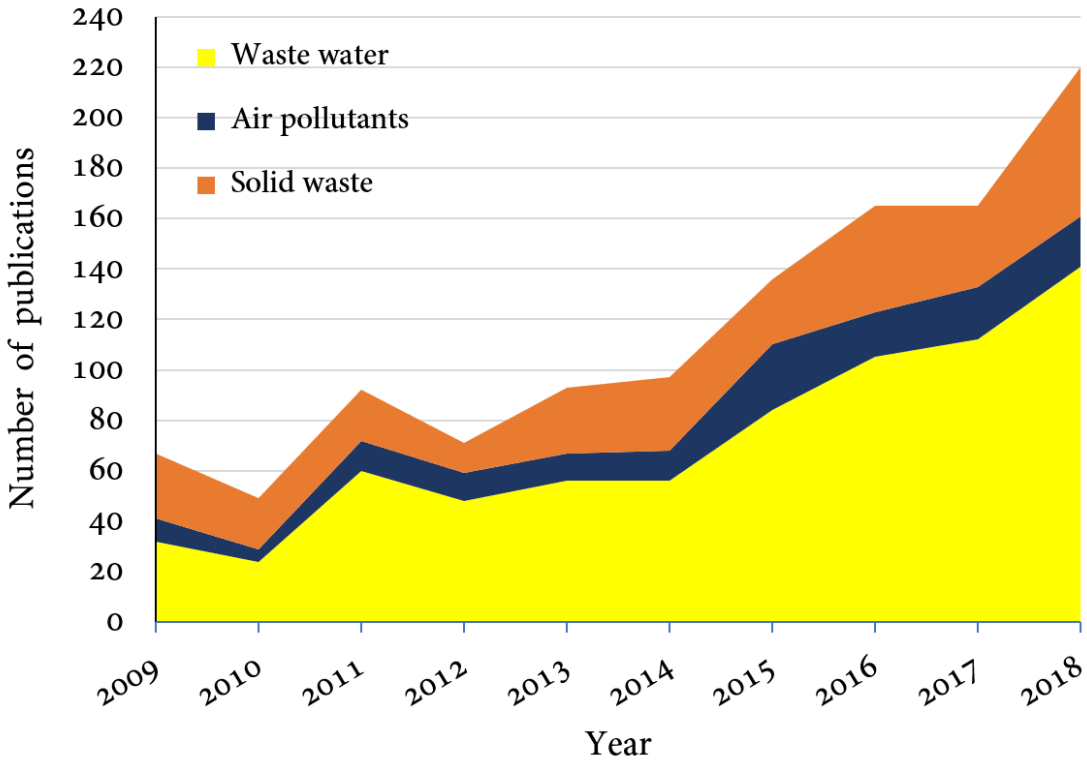

Fig. 5. Time evolution of the number of publications according to the fields of applications, based on the ISI Web of Science.

3.1 AI technologies for wastewater treatment

In the early stages, the application of AI technologies in wastewater treatment process focused on pollutants removal such as heavy metals, dyes, persistent organic pollutants, nutrients and other pollutants (Fan et al., 2018), and adsorption of various dyes from solution (Ghaedi and Vafaei, 2017). However, the main work gradually shifts to advanced controls of wastewater disposal process and soft-sensors for hard-to-measure parameters. All of these researches using AI models for wastewater treatment process will be detailed discussed in following section (Table 2-4).

3.1.1 Modeling and optimization of the pollutant removal processes

Over the past decade, AI technologies especially ANNs have emerged as high-efficiency tools for pollutant removal modeling and optimization in wastewater since their self-learning and self-adapting abilities. As shown in Table 2, the obtained results made it clear that AI technologies, especially ANNs, were widely applied to this field, mainly the removal of dyes and heavy metals. It is notable that initial concentrations of target pollutants (dyes and heavy metals), pH, contact

time and adsorbents dosages are considered as important influencing factors and also used as inputs of neural networks, removal efficiencies of target pollutants are taken as outputs (Dil et al., 2017; Dolatabadi et al., 2018; Nag et al., 2018). Generally, MLPNN is chosen as a prediction model to obtain output values based on input conditions, and BP is widely used as a training function (Antwi et al., 2018; Khandanlou et al., 2016). However, comparative studies indicate that RBFNN is a more flexible and rather effective choice for simulation and optimization of heavy metal ions and dyes adsorption processes (Asfaram et al., 2017; Messikh et al., 2015; Singh et al., 2013; Turan et al., 2011). Compared to MLPNN, the predicted removal efficiencies obtained by RBFNN are more accurate since its modular network structure and unsupervised learning characteristics.

In a study conducted by Yu et al. (2014), a batch of MLPNN models, i.e. BP-ANN, with important input variables, such as monitored pH, dissolved oxygen (DO), and oxidation-reduction potential (ORP), initial Cr(VI) concentrations, nanoscale zero-valent iron (nZVI) dosages and contact time, were applied to evaluate the removal efficiencies of Cr(VI) in the process of nZVI. Three probes monitoring the variations in DO, ORP, and pH were installed in the nZVI batch reactor, and online data was acquired. Hence, the datasets built from the batch Cr(VI) removal experiments were selected randomly as testing and training subsets. It was indicated that the well-trained MLPNN models presented precise results, exhibiting the potential to optimize the nZVI process for the removal of Cr(VI). Dolatabadi et al. (2018) employed a 5-7-2 MLPNN model and an ANFIS to predict the adsorption ability of sawdust in simultaneous removal of Cu(II) and Basic Red46 (BR46) from contaminated solution. Experimental data from 50 samples (38 samples for training, 6 samples for validation and 6 samples for testing) were applied for establishing prediction models. The results showed that both of MLPNN and ANFIS models obtained excellent predictive results (R^2 values of 0.98-0.99) for both copper and dye. In another research of Cu(II) adsorption (Khandanlou et al., 2016), 20 experimental data (15 for training and 5 for testing) were used to develop the MLPNN. It was found out that even using a small amount of data for ANN training, the estimating of adsorption efficiency of Cu(II) (74.04%) is close to the actual value of 75.54% under the obtained optimum conditions, suggesting the model can produce accurate prediction without abundantly experimental data.

433 **Table 2** Different AI models and machine learning algorithms for applications in wastewater pollutant removal processes.

NO.	Input parameters	Output parameter(s)	AI method(s)	Datasets partition			Errors (PERFORMANCE EVALUATION CRITERIA)		Ref.
				Training datasets	Validation datasets	Testing datasets	R^2	RMSE	
1	Initial Cd(II) concentration, pH, adsorbent dosage and contact time	Cd(II) removal efficiency	GA-ANN	65	19	9	0.94	0.989	Nag et al. (2018)
2	Initial Cr(VI) concentration, pH, ORP, DO, and contact time	Cr(VI) removal efficiency	MLPNN	–	–	–	0.9877	–	Yu et al. (2014)
3	Initial BR46 and Cu(II) concentrations, pH, contact time, and adsorbent dosage	Cu(II) and BR46 adsorption efficiencies	MLPNN ANFIS	38	6	6	0.9871 (Cu(II), MLPNN) 0.999 (Cu(II), ANFIS)	1.248 (Cu(II), MLPNN) 0.353 (Cu(II), ANFIS)	Dolatabadi et al. (2018)
4	Initial Pb(II), contact time, pH and adsorbent dosage	Pb(II) removal efficiency	GA-ANN	19	3	3	0.999	0.374	Yasin et al. (2014)
5	Concentrations of complexing agent and eluent, pH, amount of tea waste, eluent volume and eluent flow rates	Removal efficiencies of Mn(II) and Co(II)	PSO-ANN	76%	12%	12%	0.9807 (Mn(II)) 0.9838 (Co(II))	0.10 (Mn(II)) 0.05 (Co(II))	Khajeh et al. (2017)
6	Initial pH, adsorbent dosage, temperature and contact time	Cu(II) removal efficiencies	RBFNN	50	–	50	0.999	0.0125	Turan et al. (2011)
7	Initial concentrations of Cd(II) and MB, adsorbent mass, pH and contact time	Cd(II) and MB removal efficiencies	MLPNN BRT	36	8	8	0.9896 (MLPNN) 0.9912 (BRT)	0.0048 (MLPNN) 0.0036 (BRT)	Mazaheri et al. (2017)
8	Initial As(III), pH, contact time, temperature, material dose and agitation speed	As(III) removal efficiency	MLPNN	63	–	42	0.975	0.541	Mandal et al. (2015)
9	Initial ion concentration, adsorbent dosage, and removal time	Adsorption of Pb(II) and Cu(II)	MLPNN	15	–	5	0.9905 (Pb(II)) 0.9632 (Cu(II))	0.95 (Pb(II)) 1.87 (Cu(II))	Khandanlou et al. (2016)
10	Collector concentration, frother concentration, pH, impeller speed and flotation time	Removal efficiencies of Ni(II) and water	GA-ANN	54	–	13	0.974 (Ni(II))	0.208 (Ni(II))	Hoseinian et al. (2017)
11	Initial Pb(II) and MG, materials dosage, pH and ultrasonication time	Pb(II) and MG removal efficiencies	MLPNN	20	6	6	0.9997 (Pb(II)) 0.9999 (MG)	0.0316 (Pb(II)) 0.0632 (MG)	Dil et al. (2017)
12	Initial concentration of CV, adsorbent dosage, pH and sonication time	Adsorption of CV	MLPNN	75%	–	25%	0.9998	0.031	Dil et al. (2016)
13	Initial CG concentration, adsorbent mass and sonication time	CG removal efficiency	RF	–	–	–	0.9315	0.067	Bagheri et al. (2015)
14	Adsorbent mass, pH, sonication time, initial MB and MG concentrations	MB and MG removal efficiencies	MLPNN RBFNN	46	10	10	0.9785 (MB, MLPNN) 0.9984 (MB, RBFNN)	0.0030 (MB, MLPNN) 0.0022 (MB, RBFNN)	Asfaram et al. (2017)
15	Initial MB concentration, adsorbent mass, pH and sonication time	MB removal efficiency	LS-SVM	75%	–	25%	0.9995	0.000162	Asfaram et al. (2016)
16	Initial MB and MG concentrations, pH, adsorbent mass	Removal efficiencies of MB	MLPNN	70%	15%	15%	0.9997 (MB)	0.0245 (MB)	Asfaram et al.

	and ultrasonication time	and MG					0.9990 (MG)	0.0346 (MG)	(2016b)
17	Initial MO concentration, adsorbent dosage and contact time	MO removal efficiency	PSO-ANN	270	–	90	0.97	0.03	Agarwal et al. (2016)
18	Initial IC and SO concentrations, adsorbent mass and sonication time	IC and SO removal efficiencies	MLPNN	70%	15%	15%	0.9991 (IC) 0.9997 (SO)	0.00792 (IC) 0.00746 (SO)	Dastkhoon et al. (2017)
19	Initial BG concentration, amount of ZnS-NP-AC and contact time	BG removal efficiency	PSO-ANN	252	–	108	0.9558	0.0458	Ghaedi et al. (2015)
20	Initial concentrations of MG, DB and MB, adsorbent mass and sonication time	Removal efficiencies of MG, DB and MB	MLPNN	70%	15%	15%	0.9989 (MG) 0.9992 (DB) 0.9993 (MB)	0.0077 (MG) 0.0010 (DB) 0.0047 (MB)	Bagheri et al. (2016)
21	Adsorbent dosage, initial concentrations of EY and contact time	Removal efficiency of EY	GA-ANN	252	54	54	0.9991	0.0122	Assefi et al. (2014)
22	Initial MG concentration, contact time, pH and adsorbent dosage	Adsorption of MG	GA-SVR	176	–	75	0.9195	0.0583	Ghaedi et al. (2016)
23	Initial concentrations of BG and EB, adsorbent dosage and contact time	Removal efficiencies of BG and EB	MLPNN	41	–	13	0.9589 (BG) 0.9455 (EB)	0.0458 (BG) 0.0469 (EB)	Jamshidi et al. (2016)
24	Initial concentration of MO and contact time	Adsorption of MO	MLPNN	60%	20%	20%	0.998	10.08	Tanhaei et al. (2016)
25	Initial concentration of CV, temperature, pH, contact time and amount of magnetic activated carbon	Adsorption of CV	MLPNN	26	–	6	0.998	–	Salehi et al. (2016)
26	Initial pH, sulfate concentration, operating temperature, and adsorbent dosage	Phosphate removal efficiency	MLPNN	75%	25%	–	0.9931	–	Zhang and Pan (2014)
27	Adsorbate concentration, pH, temperature and contact time	2-chlorophenol removal efficiency	RBFNN	320	160	160	0.96	2.46	Singh et al. (2013)
28	Influent pH, COD, NH_4^+, VFA, OLR and biogas yield	COD removal efficiency	MLPNN	152	33	33	0.87	–	Antwi et al. (2018)
29	MLSS, HRT and contact time	COD removal efficiency	MLPNN	70%	15%	15%	0.9999	0.1486	Hazrati et al. (2017)
30	Initial triamterene concentration, contact time, pH, temperature and adsorbent concentration	Triamterene removal efficiency	GA-ANN	45	–	19	0.9856	0.0224	A. M. Ghaedi et al. (2016)
31	Initial pH, WTR dose, dye concentration and final pH	Color removal efficiency	RSM-ANN	60%	20%	20%	0.972	0.4	Gadekar and Ahammed (2019)
32	Initial naphthalene concentration, salinity, fluence rate, temperature and contact time	Naphthalene removal efficiency	MLPNN	116	38	38	0.943	0.042	Jing et al. (2014)
33	Initial pH, $[H_2O_2]/[Fe^{2+}]$ mole ratio and Fe(II) dosage	Mass content ratio and mass removal efficiency of COD	MLPNN	11	3	4	0.984 (MCR) 0.968 (MRE)	1.54 (MCR) 1.86 (MRE)	Sabour and Amiri (2017)

34	Precipitant dosage, pH and conductivity of the solution	Sulfate ions removal efficiency	MLPNN	70%	15%	15%	0.9955	–	Kartic et al. (2018)

In fact, there are no strict standards for the amount of the experimental data needed to train a prediction model for reliable prediction results. As seen in Table 2, datasets in some studies only included subsets of training and testing without the validation subsets. For instance, based on a dataset including 270 experimental data of training and 90 data of testing, Agarwal et al. (2016) presented a PSO-ANN to investigate adsorption of methyl orange (MO) from contaminated solutions. Ghaedi et al. (2016) combined SVR and GA to forecast malachite green (MG) adsorption using multi-walled carbon nanotubes. The dataset used in their research was divided into training (176 samples) and testing subsets (75 samples). Both of the AI models were proved to be effective and accurate tools for dye removal prediction without the validation subsets.

Meanwhile, the feasibilities of RSM, MLPNN and RBFNN models on predicting the adsorption of MG and methylene blue (MB) onto a novel adsorbent were investigated by Asfaram et al. (2017). RBFNN model was proved to be best predictive model with the highest R^2 and lowest RMSE. Singh et al. (2013) presented MLPNN, RBFNN and other three different nonlinear AI models to estimate the adsorption of 2-chlorophenol (CP) in solution using the severely nonlinear data. The RBFNN model was found to have the best predictive and generalization abilities comparing to other models. Additionally, similar conclusions have been reached according to Turan et al. (2011).The better predictive ability of the RBFNN was found than using MPNN model on adsorption of copper from industrial leachate by pumice. Owing to the ability to map principles with a high tolerance of input noises, RBFNN has been confirmed to be a preferred ANN model for removal prediction of heavy metal ions and dyes, even though more data are required for training (Buyukyildiz and Kumcu, 2017).

The applications of AI technologies in this field are not restricted to predicting and optimizing removal efficiencies of various heavy metal ions and dyes, but also nutrients, persistent organic pollutants (POPs), chemical oxygen demand (COD) and other pollutants, as seen in Table 2 (Antwi et al., 2018; Gadekar and Ahammed, 2019; A. M. Ghaedi et al., 2016; Hazrati et al., 2017; Jing et al., 2014; Kartic et al., 2018; Sabour and Amiri, 2017; Singh et al., 2013; Zhang and Pan, 2014). For example, a three-layered BP-ANN model was developed by Antwi et al. (2018) to evaluate COD removal in industrial starch processing wastewater treatment by upflow anaerobic sludge blanket reactor (UASB). Based on the PCA, six important anaerobic process parameters

such as organic loading rate, NH_4^+-N, influent pH, COD, biogas yield and effluent volatile fatty acid were selected as input variables. Without detailed mechanisms of the anaerobic process, the nonlinear behavior between these dependent and independent variables associated with anaerobic digestion process was modeled and estimated by the proposed BP-ANN model. The experimental dataset could agree well with the predicted dataset with an R^2 of 0.87, suggesting the efficacy of the BP-ANN model was able to explain at least 87% of the variation existed in the overall COD removal dataset. For the treatment of naphthalene in marine oily wastewater by the means of photodegradation, Jing et al. (2014) employed an MLPNN to simulate the removal process. The effects of operating variables on naphthalene removal were investigated. All the variables were found to have promoting effects on the removal process. The most influential parameters were found to be the temperature and fluence rate. The results of this work indicated that ANN modeling can effectively estimate the behavior of the photo-induced polycyclic aromatic hydrocarbon (PAH) removal process.

Moreover, Zhang and Pan (2014) developed RSM and MLPNN model to predict the removal of batch and column phosphate by nano-hydrated ferric oxide, and GA was applied to achieve optimal conditions. Al-Obaidi et al. (2018) employed species conserving genetic algorithm (SCGA) in optimizing a multistage reverse osmosis (RO) conditions with permeate reprocessing and recycling for the degradation of N-nitrosodimethylamine (NDMA). By the means of optimization process, the best operating configuration was found in terms of the processes of rejection, recovery and energy consumption. A. M. Ghaedi et al. (2016) employed a GA-ANN to evaluate the potential usages of single-walled and multi-walled carbon nanotubes for rapid Triamterene adsorption. The conditions including adsorbent dosage, contact time and initial dye concentration were simulated to search the best adsorption capacities of adsorbents by GA. It was concluded that under the optimizing parameters obtained by GA, the maximum adsorption capacities of single-walled and multi-walled carbon nanotubes for the Triamterene removal was 25.77 $mg \cdot g^{-1}$ and 33.14 $mg \cdot g^{-1}$ respectively.

3.1.2 Intelligent control of wastewater treatment

AI models combined with automatic control techniques of wastewater treatment process to build intelligent control strategies or systems have been widely discussed in recent reports, and

most works focused on intelligent control of aerobic stage of wastewater treatment process, to reduce total aeration time and save cost on the premise of meeting effluent standards (Asadi et al., 2017; Foscoliano et al., 2016; Ruan et al., 2017; Sun et al., 2017; Wen et al., 2017). On-line DO controlling is one of the essential parts of intelligent control as shown in Table 3. Notably, FL based intelligent control systems such as FNN and ANFIS controllers have received increasing attentions and been broadly used to achieve better effluent quality and higher cost-effective in the processes of biological wastewater treatment (Huang et al., 2009; Qiao et al., 2018; Ruan et al., 2017; Shamiri et al., 2015; Zhang et al., 2016).

Wen et al. (2017) designed a real-time DO intelligent control system consisting of a feedforward controller based on an RBF network and an improved proportion integral differential (PID) controller built on a BP network. Specifically, the proposed system contains two controlling systems, i.e. feedforward and feedback. The former system is able to obtain setting optimizing input values for feedback control system, then the latter one could ensure the stable qualified effluent through precise real-time control of DO concentration, exhibiting the feasibility of intelligent control system for wastewater treat plants (WWTPs). Ding et al. (2011) adopted a novel intelligent control system (ICS) to optimize the operation of conventional sequencing batch biofilm reactor (SBBR) in terms of the aeration process. With regard to the effects on the activity of the microorganisms, three key variables (DO, temperature and intermittent aeration) were selected as controlling factors in this proposed SBBR with ICS. Compared with traditional SBBR, the proposed system reduced the total aeration time and HRT by 50% and 56%, respectively, meanwhile achieved higher efficiency of COD removal.

Generally, aeration is regarded as the most energy-consuming part of the wastewater treatment process. It was reported that aeration could reach 50–75% of the total energy expenditure in WWTPs (Gude, 2015; Longo et al., 2016). Unlike other biochemical processes, in fact, one of the characteristics of WWTPs is large time-varying disturbances, as the random quality of the inlet wastewater. It is indicated that it could be difficult to propose an efficient aeration control strategy on the premise of reducing costs. However, it seems that AI-based aeration intelligent control systems provide an applicable possibility to reduce the operation costs of WWTPs.

521 **Table 3** Different AI models and machine learning algorithms for applications in intelligent controls.

NO.	Influencing factors	Control objective(s)	AI method(s)	Type of control	Process	Scale(s)	Effects (compared to conventional methods)	Ref.
1	DO, pH, and the manipulated variables of the pH/DO control from the aerobic phase	Aerobic phase length	SVM	On-line	SBR	Lab	Reduce aerobic phase length by 9.54 days	Jaramillo et al. (2018)
2	DO set-points in four bioreactors (Z2, Z3, Z4, Z5) and internal recirculation flow rate	Nitrate concentration in Z2 and ammonia concentration in Z5	RNN	On-line	ASP	Lab	Reduce effluent ammonia peaks, nitrate concentration, and energy consumption costs	Foscoliano et al. (2016)
3	Inlet copper concentration, inlet flow rate, underflow rate, solid content in underflow, pH, and temperature	ORP	FL	On-line	—	Pilot	Reduce outlet copper concentration, zinc consumption, and energy consumption	Zhang et al. (2016)
4	Errors of S_{O5} and S_{NO2} between optimal set-points and real outputs, and variations of the errors	Effluent S_{O5} and S_{NO2}	FNN	On-line	A/O	Lab	Reduce aeration energy by 7.6%	Qiao et al. (2018)
5	Concentrations of substrate, DO, and biomass	Rise time and settling time	ANFIS	On-line	ASP	Lab	Reduce rise time and settling time by 45.7% and 3.5%	Gaya et al. (2015)
6	Influent flow rate, returned sludge flow, temperature, and pH	DO, effluent COBD, TSS, TDP, TSP	MARS	On-line	ASP	Full	Reduce airflow rate by 31.4%	Asadi et al. (2017)
7	Effluent NH_4^+-N, TSS, TN, and nitrate concentration of the second tank	Internal recycle flow rate	ANFIS	On-line	ASP	Lab	Reduce concentrations of effluent NH_4^+-N and TN by 24.5% and 10.8%	Shen et al. (2014)
8	Influent NH_4^+-N, COD/N, effluent TN and water temperature	N_2O emission	MLPNN	Off-line	A/O	Full & Pilot	Reduce emission of N_2O down to 0.21% of N-load	Sun et al. (2017)
9	HRT, ORP, pH, DO, and flow rate	Effluent COD	GA-FL-WNN	On-line	A/A/O	Lab	Reduce operation cost by about 20%	Ruan et al. (2017)
10	UV fluence rate, salinity, temperature, initial naphthalene concentration, and reaction time	Naphthalene removal efficiency	GA-ANN	Off-line	AOPs	Lab	Reduce treatment cost by 20.4%	Jing et al. (2015)
11	DO, temperature, influent NH_4^+-N, COD and effluent NH_4^+-N, NO_2^--N, NO_3^--N, and COD	Inverter output frequency	RBFNN MLPNN	On-line	SNAD	Lab	Achieve high nitrogen removal efficiency and close control of oxygen supply	Wen et al. (2017)
12	Temperature, DO, influent NH_4^+-N, NO_2^--N, NO_3^--N, TN, TP, MLSS, SS, and COD	HRT, total aeration time, removal efficiency of effluent NH_4^+-N, P and COD/TOC	ICS	On-line	SBBR	Lab	Reduce HRT and total aeration time by 56% and 50%	Ding et al. (2011)
13	Influent COD, TN, inflow flow rate, pH, ORP, return mixed liquid ratio, and nitrate concentration of the last anoxic zone	Effluent COD, TN, and the operating costs	FNN	On-line	A/O	Lab	Reduce effluent COD, TN, and the operating costs by 14%, 10.5%, and 17%	Huang et al. (2014)
14	Concentrations of NO_3^-N, NO_2^-N, NH_4^+-N, flow rates, and DO	Effluent quality, operational costs and greenhouse gas emissions	FL	On-line	ASP	Lab	Improve 1.73% effluent quality index, reduced 15.47% aeration energy and 8.6% total CO_2 emission	Santin et al. (2018)
15	Inflow rate, COD, and concentration of NH_4^+-N	Airflow rate supplied by a blower for aeration	ANFIS	On-line	MBR	Pilot	Reduce almost 33% of the operation cost	Huang et al. (2009)

16	Influent coliform counts, turbidity, color, ORP, pH, and temperature	Effluent coliform counts	MLPNN	On-line	AOPs	Lab	Result in energy saving and capacity reduction of 13.2–15.7%.	Lin et al. (2012)

522

Foscoliano et al. (2016) revealed that a recurrent neural network model (RNN) was presented to capture the required input-output behavior. For predictive control algorithm, the dynamic matrix control (DMC) was selected to control the nitrogen compounds in the bioreactor. It was revealed that the pollutants such as ammonia and nitrate and the energy cost were reduced in this proposed predictive control of activated sludge process (ASP). In order to reduce the cost of anaerobic/anoxic/oxic (A/A/O) process in the treatment of papermaking wastewater, GA evolving fuzzy wavelet neural network software sensor was developed to control DO (Ruan et al., 2017). It was concluded that the operating costs was reduced by 20% while ensuring the effluent quality met standards. Based on SVM classification and features extraction, Jaramillo et al. (2018) suggested an on-line prediction of the length of aerobic reaction for nitrate compounds removal by closed-loop controlling the value of pH and DO. Aiming to determine the end-point of the aerobic process, a decision rule between the completion state of NH_4^+-N degradation and the NH_4^+-N degradation state was generated by using an SVM classifier. The results showed that the suggested strategy allowed for a total decrease in aerobic process lengths of 7.52% (corresponding to 9.54 days).

Although with a disadvantage of high dependence on the training data quality, fuzzy logic control systems (e.g., FNN and ANFIS) have been proved to be a remarkably superior tool to construct the strategy of multi-objective optimal control. Owing to the fuzzy rules generated by fuzzy logic with its capability to handle uncertainty, the fuzzy control systems can achieve better effluent quality on biological wastewater treatment processes (Huang et al., 2009; Kalogirou, 2003; Mohd Ali et al., 2015; Qiao et al., 2018; Ruan et al., 2017).

To realize the optimal control of DO and nitrogen nitrate concentration, Qiao et al. (2018) presented a multi-objective optimal control strategy, consisting of a control module with an FNN and the adaptive multi-objective differential evolution (AMODE) algorithm for optimization. Setting DO concentration in the 5^{th} tank (S_{O5}) and the nitrogen nitrate concentration in 2^{nd} anoxic tank (S_{NO2}) were optimized by the means of AMODE algorithm. The objective of FNN was to adjust the setting values of S_{O5} and S_{NO2} for better control results. It is noteworthy that in spite of the satisfactory of tracking performance, it is necessary to consider the stability of multi-objective control before the industrial applications. Huang et al. (2014) suggested an integrated FNN control

552 system to eliminate nitrogenous compounds at low energy cost in an anoxic/oxic (A/O) process.
553 The proposed system consists of an FNN estimator to predict the nitrate concentration in the final
554 anoxic process and FNN controller for controlling the nitrate recirculation flow. In comparison to
555 the implementation with nitrate recirculation flow rate, the operating costs, and the concentrations
556 of COD and TN for one week decreased by 17%, 14%, and 10.5%, respectively. Besides, to
557 reduce greenhouse gas (GHG) emissions, effluent nutrient concentration and operational costs in
558 WWTPs, Santin et al. (2018) designed a fuzzy controller coupled with three proportional-integral
559 (PI) controllers to optimize six variables and their time derivatives in some cases, to investigate
560 their trends over time.

561 ANFIS is another feasible technique of fuzzy control applied to wastewater treatment processes
562 (Gaya et al., 2015; Huang et al., 2009; Shen et al., 2014). It integrates learning capacities of ANN
563 and reasoning abilities of FL to map the input-output relationships. For example, Huang et al.
564 (2009) presented an ANFIS controller to adjust aeration in an aerated submerged biofilm
565 wastewater treatment process at a small-scale WWTP with a daily treatment capacity of 100 m^3
566 industrial sewage. They introduced that the proposed ANFIS controller enables them to reduce the
567 operation cost by about 33%. Gaya et al. (2015) employed an ANFIS based compensation
568 controller for dissolved oxygen control in an ASP. The study indicated that the suggested
569 controller showed better settling-time and faster response in comparison to the common PID
570 controller.

571 In addition to precisely controlling aeration to achieve the desired DO concentration, intelligent
572 control systems were also employed to optimize the photodegradation and other processes (Jing et
573 al., 2015, 2014; Lin et al., 2012; Zhang et al., 2016). As stated by Lin et al. (2012), a novel
574 MLPNN control strategy was developed for UV and UV-TiO_2 disinfection controls to meet the
575 limits of three total coliform for municipal sewage reclamation. The reported indicated that the
576 proposed ANN model could precisely correlate the interrelationships among multiple monitored
577 variables for both UV and UV-TiO_2 disinfection, even though it is almost impossible to use
578 existing mathematic methods. Besides, Jing et al. (2015) carried out a research related to the
579 naphthalene removal from marine oily wastewater by means of UV treatment. Hence, a
580 simulation-based dynamic mixed integer nonlinear programming (SDMINP) approach, which

integrating GA, multi-stage programming and developed simulation model, was presented for this continuous treatment process. The results illustrated that the treatment costs of the proposed approach and the single-stage optimization in a fixed 36-hour period were $9.11 and $11.45, respectively. Zhang et al. (2016) proposed an online evaluation strategy based on FL for the control of the Cu removal. The industrial-scale results indicated that the presented control strategy could not only reduce Cu concentration in outlet with low consumption of Zn, but also minimize energy consumption and stabilize the production process. As shown in Table 3, the majority of these researches are laboratory-scale. However, data such as water quality parameters and operational variables obtained from actual WWTPs are widely used to simulate intelligent control of wastewater treatment processes. All of the obtained progress is of great significance for development of control strategy, which will improve effluent quality and reduce operational costs in real WWTPs.

3.1.3 Soft-sensor technologies for WWTPs

In recent decades, the development of environmental technologies has promoted more stringent regulations and requirements for wastewater treatment (Olsson, 2012). For example, the renewal of the ammonia removal shifts to the removal of total nitrogen (TN) in China now. Hence, there is a strong desire to update the existing treatment process and upgrading of supporting equipment to meet these tight regulations (Haimi et al., 2013). On the other hand, the traditional strategies for the monitoring problems rely on the on-line and off-line analysis of primary parameters such as concentrations of nitrates, ammonia, chemical and biochemical oxygen demand, as well as other hard-to-measure variables like sludge blanket level. However, the availability of parameter values obtained through on-line analysis is always connected to high-cost investments and maintenance expense, while the results obtained using off-line analysis have the problems of time-delayed responses, which makes difficulty for real-time monitoring.

605 **Table 4** Different AI models and machine learning algorithms for applications in soft measurements.

NO.	Primary parameter(s)	Secondary parameters	Type	Process	AI method	Sample size	Errors (PERFORMANCE EVALUATION CRITERIA)		Ref.
							R^2	RMSE	
1	Effluent COD, TN and NH_4^+-N	Influent flow, COD, TN, NH_4^+-N, and reflux ratio of biofilm system, effluent COD, TN, and NH_4^+-N of anoxic biofilm reactor,	Off-line	A/O	PSO-SDAE	80	–	5.94 (COD) 1.26 (TN) 1.27 (NH_4^+-N)	Shi and Xu (2018)
2	Effluent TP	Influent DO, ORP, TSS, pH, NH_4^+-N, NO_3^--N and temperature	On-line	A/A/O	PLS-RBFNN	800	–	0.104	Zhu et al. (2017)
3	Effluent BOD, COD and TSS	Influent BOD, COD, TSS, pH and temperature	Off-line	ASP	FNN	159	0.96 (BOD) 0.95 (COD) 0.94 (TSS)	1.13 (BOD) 1.67 (COD) 0.98 (TSS)	Nadiri et al. (2018)
4	Effluent BOD	Influent COD, MLSS, pH, oil and NH_4^+-N	On-line	ASP	RBFNN	360	–	0.5491	Han et al. (2011)
5	Carbonaceous BOD_5	Water temperature, precipitation, pH, raw flow, TARP flow, TKN, NH_4^+-N, NO_2/NO_3-N, BOD_5, $CBOD_5$, SS, VSS, total phosphorus and soluble phosphorus	Off-line	ASP	MLR-ANN	2364	0.584	–	Zhu et al. (2018)
6	Effluent TP and NH_4^+-N	Influent pH, ORP, DO, TSS and temperature	On-line	A/A/O	PCA-FNN	–	–	0.0982 (TP) 0.0608 (NH_4^+-N)	Han et al. (2018)
7	Effluent COD, TN and TSS	Influent flow rate, NO_3-N, NH_4^+-N, alkalinity, temperature and effluent NH_4^+-N, alkalinity	On-line	ASP	MLPNN	1120	0.90 (COD) 0.92 (TN) 0.88 (TSS)	–	Fernandez de Canete et al. (2016)
8	Effluent TP	Effluent temperature, NH_4^+-N, oil and influent oil, TP and DO in biological reactor	Off-line	ASP	SCNN	360	0.8536	0.049	Li et al. (2016)
9	Effluent SS, COD and pH	Influent temperature, pH, SS and COD	Off-line	ASP	ANFIS	160	0.92 (SS) 0.86 (COD) 0.90 (pH)	0.43 (SS) 1.48 (COD) 0.04 (pH)	Pai et al. (2011)
10	SVI values	Effluent pH, COD, TN, DO and MLSS	On-line	SBR	RSONN	220	–	0.143	Han et al. (2016)
11	COD, PO_4^{3-} and NO_3-N	Influent ORP, pH and DO	On-line	A/O	GA-FNN	–	0.990 (COD) 0.987 (PO_4^{3-}) 0.977 (NO_3-N)	24.65 (COD) 5.077 (PO_4^{3-}) 4.056 (NO_3-N)	Huang et al. (2015)
12	Effluent COD	Influent flow rate, concentration of SS and NH_4^+-N, ORP in anoxic reactor and DO in aerobic reactor	On-line	A/O	WNN	250	–	–	Cong and Yu (2018)
13	Effluent BOD	Influent COD, BOD, flowrate, oxygen for the first reactor, flowrate for inner recycle, readily biodegradable substrate for effluent and another 14 variables	On-line	A/O	RVM	527	0.94	1.296	Liu et al. (2014)

606

AI-based estimators, known as soft-sensors, have been accepted as remarkable alternatives to the conventional observers and hardware sensors for rapidly and precisely estimating the hard-to-measure parameters. As shown in Table 4, a large number of researches have conducted soft-sensing studies on various primary parameters including concentrations of ammonia (NH_4^+-N), nitrates (NO_3^--N) and total nitrogen (TN), phosphates (PO_4^{3-}) and total phosphorus (TP), chemical (COD) and biochemical oxygen demand (BOD), total suspended solids (TSS) and sludge volume index (SVI) and other water quality parameters (Cong and Yu, 2018; Fernandez de Canete et al., 2016; Haimi et al., 2015; Han et al., 2016, 2011; Mulas et al., 2011; Shi and Xu, 2018; Zhu et al., 2018). These AI models applied to soft measurement were based on the data of some secondary variables (e.g., temperature, flow rate, pH, DO and ORP) that were easily obtained through on-line instruments. Among these secondary variables, pH, temperature and DO were taken as necessary parameters in most reports.

For instance, Zhu et al. (2017) presented a soft-sensor based on RBFNN to estimate the accurate values of effluent TP on-line in an industrial-scale WWTP. The suggested monitoring system consisted of soft-sensor model and on-line instruments. Therefore, the values of pH, temperature, DO, TSS, NH_4^+-N, NO_3^--N, and ORP in the A/A/O process were monitored by instruments, and these data were consistently transmitted to the soft-sensor method. RBFNN was trained up in advance for identifying the relationships between TP and the above secondary variables. It was revealed that this monitoring system was able to estimate TP values online with predicting accuracy and computational time of 83% and 16.8s, respectively. Besides, the report also pointed out that the proposed estimator could update its parameters as the change of on-line obtained data. Cong and Yu (2018) used the sampled influent data of NH_4-N, ORP, DO, suspended solid (SS) and flow rate, which were inputs in an anaerobic reactor, and then developed an integrated approach for on-line soft measurement of effluent COD in A/O wastewater treatment process. Several Hammerstein models, approximate linear dependence (ALD) analysis, adaptive weighted fusion and wavelet neural networks (WNN), were employed in their study. The findings of this research concluded that even in the case of frequent changes in operating conditions, the proposed soft-sensor could achieve a satisfactory result. Moreover, Shi and Xu (2018) applied the deep learning neural networks, namely stacked denoising auto-encoders (SDAE) deep learning

networks, to estimate effluent COD, TN and NH_4^+-N concentrations in a biofilm system. Han et al. (2016) suggested a recurrent self-organizing neural network (RSONN) to predict the values of SVI and inspecting the occurrence of sludge bulking in the wastewater treatment process. Zhu et al. (2018) proposed a hierarchical hybrid soft-sensor method incorporating ANN, compromise programming, and multiple linear regression (MLR) to predict BOD_5 values. According to the up-to-date publications, the estimations of COD and BOD account for a large proportion in the reports related to the soft measurement of effluent parameters in WWTPs.

Notably, it is feasible to realize the soft measurement of several parameters simultaneously. However, the number of parameters estimated simultaneously in one soft-sensor system is normally limited to three, possibly because too many output variables will increase the complex of nonlinearities between the inputs and the outputs, thus affecting the prediction reliability of the AI model and increasing the computational time. Fernandez de Canete et al. (2016) presented a 70-25-15-3 double-hidden MLPNN combined with PCA for on-line soft measurement of COD, TSS and TN in the effluent of ASP system. A validation process was performed to adjust the variables of the MLPNN, beginning from off-line data of the fluent parameters. The suggested estimator was tested on an industrial-scale municipal WWTP, and satisfactory prediction results were obtained under three different weather conditions (rainy, dry, and stormy). To predict the effluent COD, BOD, and TSS simultaneously in a biological WWTP (Tabriz, Iran), Nadiri et al. (2018) developed a FL based soft-sensor using influent water quality data such as pH, temperature, COD, BOD and TSS. The obtained results showed that the R^2 value for COD, BOD and TSS in the testing subset is in the range of 0.87 to 0.98, suggesting the estimated values explained more than 87% of the actual values of these three variables.

Owing to the progresses of measurement, communication and automation technologies, modern biological wastewater treatment plants have been highly instrumented and most of the easy-to-measure secondary variables are routinely on-line acquired, providing key conditions for the practical applications of soft-sensor technologies in WWTPs. For further comprehension of soft-sensors for effluent parameters, Haimi et al. (2013) provided general guidelines for biological WWTPs soft-sensors design in their review article. They classified the reviewed soft measurement applications into four categories including on-line prediction, hardware-sensor monitoring,

process monitoring and process fault detection. Additionally, in another review of the estimator applications in chemical process systems by Mohd Ali et al. (2015), the exploiting principles of soft-sensors were outlined. According to which, the first step is to understand the behavior of the process, followed by the determination of estimated parameters (e.g. concentration, temperature, and pressure) and the selection of suitable AI technologies. A guideline for researchers to choose appropriate AI methods for specific soft-sensors was also provided by a discussion of the strengths, limitations, practical implications and comparisons among different AI technologies.

3.2 Applications of environmental early-warning and assessment

3.2.1 Early-warning and assessment of aquatic environment

As a novel and efficient modeling and forecasting tool, AI technology has been gaining popularity for the aquatic environment warning and water quality assessment in rivers, lakes, oceans, as well as groundwater. As shown in Table 5, the latest studies emphasized on risk mapping of flood susceptibility using data-based AI technologies (Bui et al., 2019; Costache, 2019; Hong et al., 2018a, 2018b; Khosravi et al., 2018; Zhao et al., 2019). Identifying flood susceptible areas, assessing the distribution and magnitude of floods are crucial aspects for suggesting proper timely mitigation strategies and management of flood hazards. Although the multiple geo-environmental variables, the varying climatic condition and human factors make it rather difficult to forecast the occurrence of flash-flood locations, flood susceptibility mapping can be done with the aid of SVM, DT, ANFIS, and other AI models. The efficiencies of these models were generally evaluated by the receiver operating characteristic curve (ROC) and the area under ROC curve (AUC). Specifically, the ROC curve is a graph that illustrates the capacity of a performed statistical model to accurately forecast the occurrence of a flood event (Costache, 2019; Hong et al., 2018a). Higher AUC values stand for better prediction abilities of the susceptible models (Bui et al., 2019; W. Chen et al., 2017).

689 **Table 5** Different AI models and machine learning algorithms for applications of early-warning and assessment in the aquatic environments.

NO.	Input parameters	Output parameter(s)	AI method(s)	Datasets partition			Errors (PERFORMANCE EVALUATION CRITERIA)		Ref.
				Training datasets	Validation datasets	Testing datasets	R^2 (AUC)	RMSE	
1	Slope angle, aspect, hydrological soil group, lithology, land use, topographic position index, topographic wetness index, convergence index, profile curvature, and plan curvature	Flash-flood potential index	SVM	70%	30%	–	(AUC = 0.724–0.904)		Costache (2019)
2	Annual maximum daily precipitation, distance to road, normalized difference built-up index, drainage density, distance to river, topographic wetness index, slope, elevation, and frequency of heavy rainstorms	Flood susceptibility maps	WELLSVM	70%	–	30%	(AUC = 0.82)		Zhao et al. (2019)
3	Ground slope, normalized difference vegetation index, topographic wetness index, stream power index, lithology, river density, distance from river, rainfall, land use, altitude, and curvature	Flash-flood susceptibility maps	DT	70%	30%	–	(AUC = 0.811–0.996)		Khosravi et al. (2018)
4	Slope, normalized difference vegetation index, land use, soil type, lithology, distance to rivers, rainfall, topographic wetness index, stream power index, sediment transport index, curvature, altitude, and aspect	Flood susceptibility maps	DE-ANFIS GA-ANFIS	70%	–	30%	(AUC = 0.852 (DE-ANFIS)) (AUC = 0.849 (GA-ANFIS))		Hong et al. (2018a)
5	Lithology, distance from river network, profile curvature, plan curvature, sediment transport index, stream power index, topographic wetness index, slope angle, elevation, and soil cover	Flood susceptibility maps	FL-SVM	70%	30%	–	(AUC = 0.9865)		Hong et al. (2018b)
6	Monthly SSL data, rainfall, stage, and river discharge	Monthly suspended sediment load	CART	70%	30%	–	0.74	–	Choubin et al. (2018)
7	Monthly streamflow and SSL data	Monthly suspended sediment load	MARS	80%	–	20%	0.8923	3592	Yilmaz et al. (2018)
8	Daily flow measurement Q_t, Q_{t-1}, Q_{t-2}, daily suspended sediment load S_{t-1}, S_{t-2}	Suspended sediment load S_t	ε-SVR	312	–	134	0.868	0.68	Buyukyildiz and Kumcu (2017)
9	Daily measurements of chlorophyll-a and DO	Chlorophyll-a and DO	VMD-CEEMDAN-ELM	254	54	55	0.986 (Chl-a) 0.999 (DO)	0.064 (Chl-a) 0.051 (DO)	Fijani et al. (2019)
10	Historical TP time series	TP	WNN	64%	–	36%	–	–	Shi et al. (2018)
11	Depth of groundwater, net recharge, aquifer media, solid media, topography, impact of vadose zone and conductivity	Groundwater risk maps	ELM-MARS-SVR-M5-ANN	70%	10%	20%	0.8981	6.7	Barzegar et al. (2018)
12	Depth to water, net recharge, aquifer media, soil media, topography, vadose zone media, and hydraulic conductivity	Groundwater TCE sensitivity	DT	70%	–	30%	–	–	Yoo et al. (2016)

13	Anthropogenic, climatic, soil, and geological factors	Groundwater As contamination	RF	1178	–	295	0.71	0.01	Bindal and Singh (2019)
14	Concentrations of Fe, Pb, Cr, Cd, Mo, N, Al and Na, hardness, chlorine, turbidity, COD, TDS and EC	Leachate penetration	FL	75%	–	25%	0.99998	116	Bagheri et al. (2017)
15	Thirteen water quality variables and one hydrological variable	Arsenic concentration in a river	ANFIS	30	3	4	–	0.0059	Chang et al. (2014)
16	Wind velocity, wind direction, inflow, outflow, upstream stage, downstream stage, average distance of block from control structures and average biomass density	Flow magnitude and flow direction	MLPNN	80%	10%	10%	0.90 (Magnitude) 0.49 (Direction)	0.59 (Magnitude) 9.56 (Direction)	Chang et al. (2015)
17	Past Escherichia coli concentration, rainfall, solar radiation, tide level, water temperature, salinity, and onshore wind speed	Natural logarithm of Escherichia coli concentration	MLPNN	60%	20%	20%	–	2.008 (BW) 1.746 (DW) 1.594 (NC) 1.638 (SIL)	Thoe et al. (2012)
18	Monthly inflow-lost flow, precipitation, evaporation and outflow	Values of change in water level	ε-SVR	80%	–	20%	0.9988	0.01	Buyukyildiz et al. (2014)

690

691 Costache (2019) carried out a study on flash-flood susceptibility assessment and mapping in the
692 basin of Prahoa river, Romania. In order to calculate the potential for flash-floods occurrence, a
693 260 km^2 area was divided into training (70%) and validation areas (30%), ten hydrologic,
694 lithologic and morphologic parameters (e.g., slope angle, aspect, hydrological soil group, land use,
695 topographic wetness index, etc.) were selected through statistical analysis and integrated into four
696 different hybrid models namely Support Vector Machine-Weights of Evidence (SVM-WoE),
697 Support Vector Machine-Frequency Ratio (SVM-FR), Logistic Regression-Weights of Evidence
698 (LR-WoE) and Logistic Regression-Frequency Ratio (LR-FR). Considering the presence of the
699 surfaces previously affected by torrential phenomena, the results of this study indicated that more
700 than 33% of the evaluated areas were characterized by the high and very high flash-flood potential.
701 The comparison of the four hybrid models showed that all of these models achieved satisfactory
702 prediction results (AUC values of 0.724-0.904) with the accuracies ranging from 0.708 to 0.801
703 for both training and validating areas. Similar data-based hybrid models have been introduced and
704 also proved to be feasible and efficient according to some studies on flood susceptibility
705 assessment and early-warning in the areas of different countries such as Vietnam (Bui et al., 2019),
706 Iran (Khosravi et al., 2018), and China (Hong et al., 2018a, 2018b; Zhao et al., 2019).
707 As seen in Table 5, monitoring and early-warning of surface water quality parameters account
708 for another important subject among these recent works. For instance, based on a total of 363
709 collected measurements of chlorophyll-a (Chl-a) and DO, Fijani et al. (2019) designed a hybrid
710 framework integrating two-layer decomposition method with extreme learning machines (ELM)
711 for estimating important water quality parameters (Chl-a and DO) in a Lake reservoir. Shi et al.
712 (2018) proposed an integrating method of WNN model and high-frequency surrogate
713 measurements for anomaly detection of water quality in a rapid way. The results suggested that the
714 proposed method can successfully tell two anomaly events of TP variations with a scale of 15
715 minutes using high-frequency on-line ANN sensors.
716 Suspended sediment load (SSL) is used as a critical indicator to evaluate the influence of water
717 quality researches, land use changes and engineering practices in watercourses. Direct
718 measurement of SS is believed to be the most credible method, but the cost limits the application
719 at all gauging stations. Nowadays, AI prediction models have been developed to estimate SSL in

some rivers (Buyukyildiz and Kumcu, 2017; Choubin et al., 2018; Nourani et al., 2019; Sharghi et al., 2019; Yilmaz et al., 2018). For example, Buyukyildiz and Kumcu (2017) concluded that three variables were found to be the best input combinations, i.e. current day's flow, previous day's flow and previous SSL data. Based on this conclusion, the findings of Yilmaz et al. (2018) indicated that the data of current day's flow was remarkably effective in forecasting SSL among these three input variables. The findings of these works also suggested that the AI models were superior to conventional methods such as correlation coefficient analysis and classical regression analyses.

In additional to the uncontaminated water bodies, some works focused on verifying the applicability of AI technologies in the assessment and early-warning of the contaminated rivers (Chang et al., 2014; Liu and Lu, 2014), groundwater (Bagheri et al., 2017; Bindal and Singh, 2019; Yoo et al., 2016), lakes (Garcia Nieto et al., 2019; Li et al., 2017) and oceans (Thoe et al., 2012; Wei et al., 2015). The pollution levels and water quality parameters of natural water bodies (including polluted water bodies) are generally affected by numerous natural and human factors. Obtaining early-warning information and assessment results based on various input conditions, and exploring the influence of each factor on water bodies to determine the primary factors are key points of relevant researches.

For assessment of arsenic (As) concentration in a river of northern Taiwan, Chang et al. (2014) used monthly monitoring data to develop AI prediction models. The dataset consisted of 37 datasets of one-month antecedent rainfall (R) from a rainfall gauge station, and 13 water quality parameters collected at a water quality monitoring station each month for three years. A nonlinear factor analysis method, namely Gamma test (GT), was selected. Only three variables (R, nitrite nitrogen (NO_2^--N), and temperature (T)), which were most highly correlated factors with As concentration, were extracted from the 14 effective variables. These three variables were thus selected as input variables for an ANFIS prediction model (ANFIS-GT). Another two models namely ANFIS-CC and ANFIS-all were developed for comparisons. The input selections of ANFIS-CC were T, R and cadmium (Cd) based on the correlation analysis. While those of ANFIS-all were all the 14 variables. It was reported that ANFIS-GT model outperformed ANFIS-CC and ANFIS-all model with 50 and 52% improvements in RMSE, respectively, because the selections of input variables were more reasonable by using GT. On the other side, importance

assessment of influencing factors affecting As concentration suggested that low temperature, high nitrite nitrogen concentration and large one-month antecedent rainfall would lead to high arsenic concentration in surface water.

In reports related to the assessment of contaminated groundwater, Yoo et al. (2016) integrated decision tree (DT) and ruled induction to predict patterns of groundwater pollution sensitivity. The data samples were collected from a trichloroethylene (TCE) contaminated site from the Woosan Industrial Park in South Korea. The author revealed that net recharge, aquifer media and soil media were the main hydrogeological parameters affecting the sensitivity of groundwater to TCE. Bagheri et al. (2017) employed FL, MLPNN and RBFNN to simulate the infiltration process of landfill leachate, the developed models were applied to predict and evaluate the environmental impact of leachate penetration. The results indicated that Mo, Na and COD are the three most influencing variables for leachate penetration into groundwater. Besides, Thoe et al. (2012) conducted a comprehensive research to predict the next-day bacterial concentration in four selected beaches in Hong Kong. Both the presented MLR and ANN estimators outperformed the current beach strategies in tracking water quality parameters and estimating water quality objective exceedances. Compared to MLR, the ANN estimator is good at estimating the high-end concentrations, but has more false alarms (false positive predictions). The issue was possibly caused by the deficiency of routine monitoring data in extreme conditions (such as strong winds, typhoons or rainstorms).

3.2.2 Analysis and forecast of pollutant concentration in the atmospheric environment

It was reported that series of AI models have been used to estimate air pollutants (Bunsan et al., 2013; Niu et al., 2016; Park et al., 2018; Sarigiannis et al., 2014; Voukantsis et al., 2011; Wang et al., 2018, 2015; Zhou et al., 2014) and establish air quality monitoring and early-warning systems (Li and Zhu, 2018; Wang et al., 2017; Yang and Wang, 2017). Large amounts of historical data were required to develop AI models for analyzing and forecasting various atmospheric pollutants concentrations. Long-term observational datasets with a period of more than one year were fundamental for AI models training, validating and testing (He et al., 2017, 2016; Li and Zhu, 2018; Zhou et al., 2019). Given the concentrations of air pollutants have characteristics of strong time-variability and uncertainty, the reported models generally took more than 8 influencing

778 factors (such as meteorological factors and the historical concentrations of various pollutants) as
779 inputs, and the number of predicted pollutant indicators is always multiple. Although PCA and
780 other data analysis methods were widely applied to preprocess large datasets, the predictive
781 accuracy of these models was generally lower than that of the models applied to the aqueous
782 environment.
783 He et al. (2016) suggested a BP-ANN model to predict daily concentrations of PM_{10}, NO_2, and
784 SO_2 over urban Lanzhou, China. In their study, daily average PM_{10}, NO_2, and SO_2 concentrations
785 and ten meteorological parameters for six winters covering 2002–2007 were collected to constitute
786 the original dataset. According to the correlation analysis and classification of synoptic-scale
787 circulations (concluded by PCA and other pre-treatment methods), six local meteorological
788 parameters including wind speed (W_s) at 200 m, wind direction index (W_{di}) at 800 m, potential
789 temperature lapse rate (γ) at 50 m, gradient Richardson number (R_i) at 150 m, stable energy (E_w),
790 and boundary layer height (H_{pbl}), coupled with historical PM_{10}, NO_2, and SO_2 concentrations,
791 were selected as inputs of BP-ANN model. It was revealed that local meteorological conditions
792 have considerable contributions to the daily variations of pollutant concentrations. Even though
793 the relative low correlation coefficient value of 0.71 to 0.83 was achieved for daily averages of
794 PM_{10}, NO_2, and SO_2, BP-ANN still can reproduce the pollution level and diurnal variations in a
795 satisfied way. Based on the long-term historical data from 2014 to 2015 (spanning all four seasons)
796 from industrial (Pukou) and suburban (Xianlin) areas in Nanjing, China, Leng et al. (2017)
797 developed rapid prediction models to estimate size-fractionated airborne particle-bound metals.
798 Meteorological factors and PM concentrations were selected as input parameters, the
799 concentrations of fourteen different elements were taken as outputs. In this study, the prediction
800 effects of three linear and nonlinear models including SVM, BP-ANN, and MLR were compared.
801 The result showed that the SVM models were superior. The well-trained SVM models were then
802 applied to predict the daily airborne elements concentrations in 2015. The obtained results
803 indicated that higher concentrations of nearly all elements were observed in industrial areas in
804 winter compared to other seasons, which were in accordance with the data recorded in 2015.
805

806 **Table 6** Different AI models and machine learning algorithms for applications of analysis and forecast in the atmospheric environments.

NO.	Input parameters	Output parameters	AI methods	Datasets partition			Errors (PERFORMANCE EVALUATION CRITERIA)		Ref.
				Training datasets	Validation datasets	Testing datasets	R^2	RMSE	
1	Original daily AQI data series	AQI	CEEMD-VMD-DE-ELM	701	—	30	—	3.66 (Beijing) 3.27 (Shanghai)	Wang et al. (2017)
2	Historical concentrations of PM_{10}, $PM_{2.5}$, SO_2, NO_2, CO and O_3	PM_{10}, $PM_{2.5}$, SO_2, NO_2, CO and O_3	ICEEMDAN-ICA-ELM	639	—	273	0.915 (PM_{10}, Guangzhou) 0.937 (NO_2, Guangzhou)	8.1673 (PM_{10}, Guangzhou) 4.6579 (NO_2, Guangzhou)	Li and Zhu (2018)
3	Historical concentrations of SO_2, NO_2, CO, O_3, PM_{10} and $PM_{2.5}$	SO_2, NO_2, CO, O_3, PM_{10} and $PM_{2.5}$	MCSDE-CEEMD-ENN	1004	168	—	—	1.87 (SO_2, Xian) 1.91 (NO_2, Xian)	Yang and Wang (2017)
4	Vehicle specific power, acceleration, and speed of the bus in the immediate past one second	Bus emissions of CO, CO_2, HC, and NO_x	MLPNN	—	—	—	0.781	0.092	Wang et al. (2018)
5	Time-delayed $PM_{2.5}$ concentrations, humidity, temperature, wind speed, planetary boundary layer height, and AOD data	$PM_{2.5}$ concentration	CNN-LSTMNN	60%	20%	20%	—	12.08	Wen et al. (2019)
6	Daily average SO_2, PM_{10}, $PM_{2.5}$, daily minimum temperature, total precipitation, surface air relative humidity and surface wind speed	$PM_{2.5}$ concentration	EEMD-GRNN	94%	—	6%	—	29.45	Zhou et al. (2014)
7	Air temperature, relative humidity, wind speed, SPM, SO_2, and NO_2	RSPM, NO_2, and SO_2	GRNN	985	211	211	0.869 (RSPM) 0.797 (NO_2) 0.783 (SO_2)	11.35 (RSPM) 2.35 (NO_2) 1.08 (SO_2)	Singh et al. (2012)
8	Surface temperature, k-index, aerosol optical depth and relative humidity	PM_{10} concentration	MLPNN	—	—	—	0.71	11.61	Kamarul Zaman et al. (2017)
9	Five meteorological factors and eight air quality factors	$PM_{2.5}$ concentration	SVM	35064	—	26304	—	0.1322	Zhou et al. (2019)
10	Outdoor PM_{10} concentration, subway frequency and ventilation rate	PM_{10} concentrations in subway stations	MLPNN	80%	20%	—	0.80 (A2)	24.89 (A2)	Park et al. (2018)
11	Meteorological parameters, the optimal lag time, precipitation and pollutant concentrations	Daily average concentrations of SO_2, NO_2 and PM_{10}	MLPNN	80%	10%	10%	0.71 (SO_2) 0.83 (NO_2) 0.79 (PM_{10})	15.7 (SO_2) 20.1 (NO_2) 64.5 (PM_{10})	He et al. (2016)
12	Meteorological data and size-fractionated heavy metal concentrations in airborne PM	Airborne particle-bound metals (Al, As, Ba, Cd, Cr, Cu, Fe, Mn, Ni, Pb, Sr, Ti, V, and Zn)	SVM	80%	—	20%	0.82 (Ni)	1.179 (Ni)	Leng et al. (2017)
13	PM_{10} and $PM_{2.5}$ concentrations of the previous day, wind speed and direction, temperature, humidity, precipitation and one categorical variable	PM_{10} and $PM_{2.5}$	MLPNN	—	—	—	0.6991 (PM_{10}) 0.7776 ($PM_{2.5}$)	—	Sarigiannis et al. (2014)

14	Original time series of $PM_{2.5}$ concentrations	$PM_{2.5}$ concentration	CEEMD-SVR-GWO	70%	—	30%	0.84 (Harbin) 0.88 (Chongqing)	0.20 (Harbin) 0.14 (Chongqing)	Niu et al. (2016)
15	Meteorological parameters and historical concentrations of NO_2, CO, O_3, PM_{10} and SO_2	PM_{10} and $PM_{2.5}$	MLPNN	67%	—	33%	0.587 (PM_{10})	5.884 (PM_{10})	Voukantsis et al. (2011)
16	Gross domestic product, gross inland energy consumption, incineration of wood, motorization rate and six other parameters	Annual PM_{10} emissions	GA-GRNN	60%	10%	30%	0.88	3.99	Antanasijevic et al. (2013)
17	Meteorological conditions and historical average concentrations of SO_2 and PM_{10}	SO_2 and PM_{10}	ANN SVM	438	—	292	0.7942 (SO_2, HANN)	0.042 (PM_{10}, ANN) 0.064 (SO_2, ANN) 0.046 (PM_{10}, SVM) 0.074 (SO_2, SVM)	Wang et al. (2015)
18	Activated carbon injection, concentration of hydrogen chloride in the flue gas at the stack emission, temperature at the mixing chamber and temperature of final fuel gas emission	Dioxin emission	MLPNN	70%	—	30%	0.998	—	Bunsan et al. (2013)

807

Among these studies in Table 6, the researches of particulate matters (PMs) account for a large proportion (Niu et al., 2016; Park et al., 2018; Sarigiannis et al., 2014; Voukantsis et al., 2011; Zhou et al., 2014, 2019). Relevant researches have revealed that indoor PMs prediction model could be established by taking outdoor PMs monitoring data as one of the important factors. For example, Park et al. (2018) developed an ANN model for predicting PM_{10} concentrations at 6 subway stations. It's worth noting that the information of outdoor PM_{10} obtained from the nearby outdoor air monitoring sites was used due to the difficulty and high expense of collecting PM data indoor. Coupled with other indoor parameters such as subway frequency and ventilation rate, the proposed ANN model could estimate 67~80% of PM_{10} at six subway stations.

Hybrid AI-based air quality monitoring and early-warning systems for reliable and scientific air quality index (AQI) forecast have been introduced by Li and Zhu (2018) and Yang and Wang (2017). a single AI method may not be sufficient to process and analyze large amounts of pollutant data, due to the irregularity, non-stationarity and randomness of AQI. According to the study of Li and Zhu (2018), the proposed hybrid AI system consists of three stages including i) an FL-based attributes selection for the determination of main pollutants for cities, ii) a deterministic prediction part for the estimation of pollutants, iii) an uncertainty prediction for estimating the possible boundary of deterministic forecasts and tackling the uncertainty of the future AQI. The availability of this hybrid system was validated in six target cities in China, and it was successful to predict the concentrations of six core indicator such as PM_{10}, $PM_{2.5}$, SO_2, NO_2, CO, and O_3. Besides, by integrating the AQI assessment and prediction module, Yang and Wang (2017) established an AQI monitoring and early-warning system. Comparing to another ten different AI models (e.g., MLPNN, RBFNN, GRNN, ENN, etc.), the proposed model was proved to show the highest effectiveness in two studies for the estimations of the major air pollutants. In the above works, complementary ensemble empirical mode decomposition (CEEMD) was employed as a denoising technique for processing nonlinear and non-stationary time series, eliminating the effects of outliers and improving prediction accuracy. Appling FL to determine the main pollutants, and it is more and more common to use machine learning models embedded with heuristic algorithms for AQI prediction. It can be concluded that the hybrid AI methods were preferred and also confirmed to be more appropriate for establishing air quality monitoring and early-warning systems.

837 Although the prediction of most air pollutants is not so accurate, efficient forecasting can be
838 realized on the premise that the numbers of inputs and outputs are small and the dataset is properly
839 preprocessed. Bunsan et al. (2013) presented a 5–8–1 BP-ANN model to predict the
840 polychlorinated dibenzo-p-dioxins (PCDDs) emission from a municipal solid waste incinerator. In
841 their study, five key factors, including the injection of activated carbon, injection frequency, HCl
842 concentration in the flue gas at the stack emission, temperature at the mixing chamber and effluent
843 were extracted from 23 candidates by PCA, in which their percentages of variance explained
844 75.78% of the total variance in the 4-year monitoring dataset of an incinerator in Taiwan. The
845 results illustrated that the proposed BP-ANN model provided high performance in the estimation
846 of PCDDs emission with an R^2 value of 0.998 in both training and testing steps.

847 **3.3 AI technologies for solid waste management**

848 Improvement of solid waste management services and minimization of solid waste are essential
849 aspects for sustainable and habitable cities, since the hazard of solid waste can affect air quality
850 and soil security (Adeyemi et al., 2001; Esin and Cosgun, 2007; Zhou et al., 2015). AI techniques
851 have been utilized as a modeling and forecasting tool to assist simulation and optimization.
852 The latest applications mainly emphasized on solid waste generation forecast (Table 7),
853 modeling and optimization of a recycling process (Table 8).
854

855 **Table 7** Different AI models and machine learning algorithms for applications of solid waste generation forecasts.

NO.	Input parameters	Output parameter(s)	AI method(s)	Solid waste	Scale	Errors (PERFORMANCE EVALUATION CRITERIA)		Ref.
						R^2	RMSE	
1	Historical weather data, historical MSW collection data and spatiotemporal tonnage data	Weekly MSW generation tonnages	GBRT	MSW	Short-term	0.906 (Spatial) 0.889 (Spatiotemporal)	22.059 (Spatial) 21.632 (Spatiotemporal)	Johnson et al. (2017)
2	Total family income, education, occupation and type of houses	Plastic waste generation rate	ANN SVM RF	Plastic waste	Short-term	0.75 (ANN) 0.74 (SVM) 0.66 (RF)	9.53 (ANN) 9.88 (SVM) 11.22 (RF)	Kumar et al. (2018)
3	Degree of urbanization, area, number of school years attended, purchase power index, deprivation index, and four other parameters	Amount of separately-collected packaging waste	GA-ANN	Packaging waste	Mid-term	0.98	—	Oliveira et al. (2019)
4	Monthly time series of municipal solid waste generation	Municipal solid waste generation	ANFIS SVM MLPNN kNN	MSW	Short-term	0.98 (ANFIS) 0.71 (SVM) 0.46 (MLPNN) 0.51 (kNN)	175.18 (ANFIS) 231.99 (SVM) 290.55 (MLPNN) 308.19 (kNN)	Abbasi and El Hanandeh (2016)
5	Individual building attributes, neighborhood socioeconomic characteristics, weather and selected route-level collection data	Building-level municipal solid waste generation	GBRT	MSW	Mid-term	0.87	0.034	Kontokosta et al. (2018)
6	Fraction of population over 45 years, median personal income, employment rate and seven other parameters	Regional municipal solid waste generation and diversion	DT ANN	MSW	Mid-term	0.54 (DT) 0.72 (ANN)	172.8 (DT) 141.8 (ANN)	Kannangara et al. (2018)
7	Population, industrial solid waste generation, urban population percentage and gross domestic product	Quantity of industrial solid waste	ANFIS ANN	Industrial waste	Long-term	0.41 (ANFIS) 0.33 (ANN)	2316 (ANFIS) 3812 (ANN)	Tiwari and Bajpai (2012)
8	Population, solid waste collection frequency, maximum seasonal temperature and altitude	Seasonal municipal solid waste generation rate	ANN MLR	MSW	Short-term	0.74 (ANN) 0.49 (MLR)	68.32 (ANN) 95.13 (MLR)	Azadi and Karimi-Jashni (2016)
9	Twelve previous weekly waste generation time series and seasonal data	Municipal waste generation	PLS-SVM	MSW	Short-term	0.869	1541	Abbasi et al. (2013)
10	Household size, total family income, education, occupation and fuel used in the kitchen	Biodegradable MSW generation rate and non-biodegradable MSW generation rate	MLR	MSW	Mid-term	0.782 (Biodegradable) 0.676 (Non-biodegradable)	5.28 (Biodegradable) 6.5 (Non-biodegradable)	Kumar and Samadder (2017)
11	Total number of residents, native residents, native and total people aged 15-59 years, number of households, income per household, and number of tourists	Annual MSW generation	ANN	MSW	Mid-term	0.96	470.9	Sun and Chungpaibulpatana (2017)
12	Gross domestic product, domestic material consumption, urban population, population density, average household size, industry value added, tourism expenditure and five other parameters	Annual MSW generation	GRNN	MSW	Mid-term	0.981	26.4	Adamovic et al. (2017)

856 **Table 8** Different AI models and machine learning algorithms for applications of solid waste recycling and reduction.

NO.	Input parameters	Output parameters	AI methods	Datasets partition			Errors (PERFORMANCE EVALUATION CRITERIA)		Ref.
				Training datasets	Validation datasets	Testing datasets	R^2	RMSE	
1	Hydrogen peroxide concentration and temperature	Lignin content, glucose concentration, xylose concentration and oxidized lignin amount	MLPNN ANFIS	67%	—	33%	0.995 (Lignin content, MLPNN) 0.995 (Lignin content, ANFIS)	0.0245 (Lignin content, MLPNN) 0.0165 (Lignin content, ANFIS)	Rego et al. (2018)
2	Temperature, pH, agitation and time in municipal waste activated sludge pre-treatment	Enzyme activity	MLPNN	60%	20%	20%	0.990 (Protease) 0.994 (Amylase) 0.995 (Lipase)	2.081 (Protease) 1.252 (Amylase) 2.253 (Lipase)	Selvakumar and Sivashanmugam (2018)
3	Mixing ratio of textile dyeing sludge and pomelo peel, heating rates, combustion atmosphere and temperature	Mass loss percent	MLPNN RBFNN	95%	–	5%	0.9998 (MLPNN) 0.9982 (RBFNN)	0.3254 (MLPNN) 1.0778 (RBFNN)	Xie et al. (2018)
4	Biomass sludge ratio, heating rate and temperature	Mass loss percent	MLPNN	80%	–	20%	0.9999	0.482	Chen et al. (2017)
5	Gas mixing ratio, heating rate, and temperature	Mass loss percent	MLPNN	75%	–	25%	0.9998	0.381	Chen et al. (2018)
6	Mass proportions of wheat bran, type II wheat flour and sugarcane bagasse	Specific amylolytic activity	GA-ANN	70%	15%	15%	0.912	—	Fernández Núñez et al. (2017)
7	KOH concentration, extractant dose, contact time and precipitant volume	Humic acid yield	MLPNN	170	37	36	0.9947	—	Genuino et al. (2017)
8	Hot air temperature and velocity	Moisture content ratio and average temperature	MLPNN GRNN	70%	15%	15%	0.999 (MR, MLPNN) 0.988 (MR, GRNN)	0.0005 (MR, MLPNN) 0.03 (MR, GRNN)	Huang and Chen (2015)
9	Amount of tea waste, pH, concentration of PAN, sample and eluent flow rates, eluent volume and concentration of eluent	Extraction percent of Mn and Co	PSO-ANN	76%	12%	12%	0.9417 (Mn) 0.9838 (Co)	0.10 (Mn) 0.051 (Co)	Khajeh et al. (2017)
10	Carbon, hydrogen, nitrogen, sulphur, oxygen, moisture content, ash, equivalence ratio and temperature of gasifier	lower heating value of gas (LHV), lower heating value of gasification products (LHV_p), and gas yield	MLPNN	47	10	10	0.9356 (LHV) 0.9866 (LHV_p) 0.9895 (Gas yield)	0.040 (LHV) 0.045 (LHV_p) 0.030 (Gas yield)	Pandey et al. (2016)
11	Human labor, water, electricity, natural gas and transportation	Abiotic depletion potential, acidification potential and other eight environmental impact categories, and recycled materials	MLPNN	70%	15%	15%	0.973 (AD) 0.935 (AC) 0.937 (RM)	0.111 (AD) 0.100 (AD) 0.128 (RM)	Nabavi-Pelesaraei et al. (2017)
12	Human development index, gross domestic product, domestic material consumption and ten other parameters	Primary production of energy from municipal solid waste	GRNN	123	30	17	0.995	4.411	Adamovic et al. (2018)

13	Biomass loading, reaction time and particle size of biomass	Glucose and xylose concentrations	MLPNN	84	18	18	0.98	9.491	Vani et al. (2015)

857

3.3.1 Solid waste generation forecasts

Precise estimation of solid waste generation is a key for waste management planning and the further design of incentives to encourage composting and recycling. Traditional and descriptive statistical methods for solid waste quantities estimation generally adopt average per-capita waste generation and population growth as the main indicators. It seems that these methods are impractical nowadays due to the increasingly complex dynamic characteristics of solid waste generation process (Abbasi et al., 2013; Abdoli et al., 2012; Sha'Ato et al., 2007). Regression analysis and material flow model as alternatives are widely used for solve this problem. However, the input variables in regression analysis have to meet strict requirements including constant variance, independence and normality of errors, limiting its applicability in solid waste quantities estimation (Abbasi and El Hanandeh, 2016; Hockett et al., 1995). The feasibility of material flow model is also restricted since this method is unable to predict collected waste without available data of recycling and littering rates (Beigl et al., 2008).

Recently, AI technologies such as ANN, SVM, DT and ANFIS have been employed for modeling municipal solid waste (MSW) generation due to their satisfactory prediction abilities. According to the length of the forecast period, current studies usually can be divided into 3 different groups including short-term prediction (from days to months), mid-term prediction (months to 3–5 years), and long-term prediction (trying to predict many years ahead). Using historical socio-demographic, economic, and management-orientated data, most of the reported AI based models were confirmed to be promising methods, exhibiting accurate predictive MSW generation in the scales of short (Abbasi et al., 2014; Johnson et al., 2017), medium (Abbasi and El Hanandeh, 2016; Kontokosta et al., 2018), and long-term (Tiwari and Bajpai, 2012).

As shown in Table 7, Johnson et al. (2017) employed a gradient boosting regression tree (GBRT) model for short-term waste estimation in New York City. Trained on integrated historical waste collection data from 2005 to 2011, the proposed model was able to estimate weekly MSW generation quantities (including recycling of refuse, paper and metal/glass/plastic) with an average accuracy of 88% for 232 geographic sections of New York City in the year 2012. The waste collection data from the New York City Department of Sanitation (DSNY) spans more than a decade, each record contains the collection data of one truck including the collected tonnage, the

887 type of collected material and the geospatial area. Owing to the fine spatial and temporal
888 granularity of the comprehensive DSNY data, the model can successfully estimate weekly waste
889 generation. On the other hand, relevant studies have concluded that seasonal patterns act as
890 important roles in short-term MSW forecasting (Abbasi et al., 2013; Noori et al., 2010). For the
891 purpose of developing applicable prediction models for weekly MSW generation, Abbasi et al.
892 (2013) took a weekly time series with 12 lag times (equal to a full season) as model inputs.
893 Specifically, the last time series which relied upon 12 previous time series as predictors were
894 assumed as the response variable. Such kind of input variable is consistent with some other reports
895 about weekly MSW forecasting (Abbasi et al., 2014; Noori et al., 2009), so it can be inferred that
896 seasonal patterns should be taken into account when determining input variables for short-term
897 forecasting models of MSW generation.

898 Furthermore, AI based mid-term and long-term prediction models were also investigated, most
899 of which were proved to be effective with accuracy over 90% as displayed in Table 7. Kontokosta
900 et al. (2018) integrated GBRT with ANN to develop a socio-spatial model for mid-term estimation
901 of building-level waste generation for more than 750,000 residential properties in New York City.
902 The model was presented with 93.9% prediction accuracy. An ANN model was trained by
903 historical data from 2005 to 2015 to forecast MSW generation in Bangkok (Sun and
904 Chungpaibulpatana, 2017). Using PCA, main indicators such as total MSW, total number of
905 residents, number of households, number of tourists, income per household, native and total
906 people aged 15 to 59 years were identified as key variables and inputs of the ANN model. This
907 proposed model showed satisfactory predictive performance on estimating annual MSW
908 generation with an R^2 value of 0.96. However, the lack of sufficient predictor variables (e.g.,
909 weather, seasonality and urban form) in the dataset could result in model deficiency with high
910 errors and poor R^2 values. For example, based on socio-economic and demographic data of 220
911 municipalities in Canada, ANN and DT models were employed to estimate MSW generation and
912 paper diversion (Kannangara et al., 2018). The proposed models of paper diversion exhibited
913 worse performance with poorer R^2 (0.31–0.35) and higher errors (32–36%) compared to other
914 models of MSW prediction, because the socio-economic and demographic variables were
915 insufficient to describe the variation in the paper recycle rate.

Nowadays, several studies have been carried out to forecast specific solid waste generation such as plastic wastes (Kumar et al., 2018) and household packaging waste (Oliveira et al., 2019) using appropriate AI technologies. The obtained results confirmed the feasibility and efficiency of AI-based models for predicting and evaluating solid waste generation. Meanwhile, the analysis and selection of key indicator, as well as the completeness and sufficiency of datasets played a crucial role in the model prediction performance.

3.3.2 Recycling and reduction of solid waste

The increasing amount of various solid waste and the significant environmental problems caused by treatments (including thermal, mechanical, biochemical processes, etc.) have stimulated a series of new technologies (such as gasification, co-combustion, etc.) for the recycling and reduction of solid waste. Through these technologies, we can extract enzymes, fuels and other valuable resources from specific solid waste, reducing the amount of solid waste.

As promising nonlinear modeling and forecasting tools, AI-based analysis and prediction models have been applied for optimization of solid waste recycling (Fernández Núñez et al., 2017; Genuino et al., 2017; Khajeh et al., 2017; Selvakumar and Sivashanmugam, 2018) and reduction process (Chen et al., 2018; J. C. Chen et al., 2017; Pandey et al., 2016; Rego et al., 2018; Xie et al., 2018).

Genuino et al. (2017) studied the extraction of humic acid (HA) from MSW biochar in the process of chemical activation, and applied a well-trained BP-ANN to optimize the extraction process. The proposed BP-ANN model was employed for evaluating the effects of extractant dose, KOH concentration, precipitant volume and contact time on the HA yield, and the optimal value of each factor was sought by using a database of 243 experimental samples, a three-layer BP-ANN with four inputs (the four influencing factors) and one output (HA yield). The contribution of each input factor was calculated using the weights and biases of the hidden layer neurons. The result exhibited that KOH concentration had the greatest impact on the output with an importance of 54.3%, followed by precipitant volume (26.9%), contact time (10.8%) and extractant dose (8.0%). The results of verification experiments (HA yield = 187.52 $mg \cdot g^{-1}$) showed that the BP-ANN underestimated the actual yield by just 3.71%. Fernández Núñez et al. (2017) investigated the definition of culture medium composition for high level production of amylase using four

agro-industrial wastes through a hybrid GA-ANN model. Compared to RSM, the optimal composition (mixtures of 91% wheat bran and 9% soybean meal) to maximize amylase activities obtained by GA-ANN was closer to the actual experimental values. The comparative result of AI technology and RSM was also achieved by Selvakumar and Sivashanmugam (2018). In their research, a multi-hydrolytic biocatalyst (MHB), which was prepared from organic solid waste, was employed in the pre-treatment of municipal waste activated sludge. Lipase, amylase and protease activities of the obtained MHB were investigated for determining the multi-hydrolytic activity. RSM and ANN modeling were applied to validate the activity of each enzyme, it was suggested the predictive abilities of designed ANN models were higher than RSM. As a classic nonlinear modeling method, RSM has been widely compared to AI models (Antwi et al., 2018; Fernández Núñez et al., 2017; Geyikçi et al., 2012; Kartic et al., 2018; Kasiri et al., 2008; Zhang and Pan, 2014). Though the results of most related studies (Karri et al., 2018; Khajeh et al., 2013; Sabour and Amiri, 2017) concluded that AI models offered more precise predictions than RSM with higher R^2 values and smaller average errors, these two models complement each other in the interpretation of the simulated results. According to Sabour and Amiri (2017), setting RSM prior to ANN (as a feeding tool) can significantly enhance the predictive capacity of ANN. AI models are usually more effective to capture highly nonlinear relationships of the simulated results and influencing factors, while RSM models are good at describing the statistical importance of the independent influencing parameters and their interactions. One drawback of RSM is that only quadratic nonlinear correlations was considered, resulting in the requirement for extra experiments as well as good priori knowledge of a system (Fan et al., 2018; Karimifard and Alavi Moghaddam, 2018; Lingamdinne et al., 2018).

On the other hand, more researches are focusing on improving the efficiency of solid waste reduction by applying AI-based analysis and prediction. Xie et al. (2018) developed ANN models to predict thermogravimetric analysis (TGA) data under five different ratios of O_2/CO_2 for modeling and optimization of the co-combustion process of pomelo peel and textile dyeing sludge. Chen et al. (2018) investigate the thermodynamic characteristics and kinetics of coffee grounds and sewage sludge co-combustion under increased ratios of O_2/CO_2 (21, 30, 40 and 60%). A 3-20-1 MLPNN was presented to estimate mass loss percent as a function of O_2-CO_2 mixing ratio,

974 temperature, and heating rate in their study. Rego et al. (2018) applied ANN and ANFIS models
975 for optimizing the sugarcane bagasse pre-treatment using alkaline hydrogen peroxide (AHP).
976 About 75% lignin removal was achieved with the obtained optimal delignification conditions of
977 7.5% H_2O_2 solution at 45°C. It was demonstrated that AI models trained by limited experimental
978 data can establish reliable correlations between impact factors and expected results, thus helping
979 the researchers to comprehensively understand the dynamics and biochemical mechanism of the
980 multiphase system in the solid waste disposal process. It is conducive to use AI models to promote
981 the disposal process in a practical issue.

982 4. Conclusions and prospects

983 One notable development over the past decades was the popularity of artificial intelligence
984 technologies in the area of environmental pollution controls, which has been considered as
985 attractive and efficient alternative methods to tackle the complexities of uncertain, interactive and
986 dynamic environmental problems. As is shown in Fig.6, among all these technologies, various
987 types of ANNs are the most widely used AI technologies because they are much easier to
988 implement. However, the performance of ANNs is restricted since their relatively poor
989 reproducibility and limited global searching ability. As a result, with the rapid development of
990 various AI technologies, an increasing number of researchers emphasize on hybrid methods (e.g.,
991 FNN, ANFIS and GA-ANN) instead of single ones. It is clear from Fig. 7 that the studies on
992 hybrid AI methods are catching up in the last three years and it seems that these methods are on
993 the verge of overtaking single methods and become the most popular AI methods applied in the
994 fields of environment. One trend that worth noting is that increasing linear and nonlinear
995 multivariate data analysis methods (i.e., PCA (Fernandez de Canete et al., 2016; Han et al., 2018;
996 He et al., 2016), PLS (Zhu et al., 2017), MLR (Zhu et al., 2018), etc.) have been incorporated into
997 different AI models as pre-processing methods for data dimensionality reduction or feature
998 extraction. Fig. 8 summarized the types of reviewed case studies (not limited to the reported tables
999 above), showing that the main applications of AI technologies are simulation processes, except for
1000 water pollution control. The intelligent control and soft measurement of wastewater treatment are
1001 becoming new tools in practical WWTPs, the number of practically implemented works in
1002 WWTPs is even higher than simulation studies.

Overall, this review summarizes and provides a brief overview of mainstream single and hybrid AI methods applied in different environmental fields, the effectiveness of the presented AI technologies that related to water, air, and solid waste over recent decade is extensively discussed. The nonlinearity nature of ANN is able to accurately predict pollutant removal, especially widely used MLPNN that requires relatively small dataset for modeling establishment. Initial concentrations of target pollutants, pH, contact time and adsorbents dosages are generally taken as

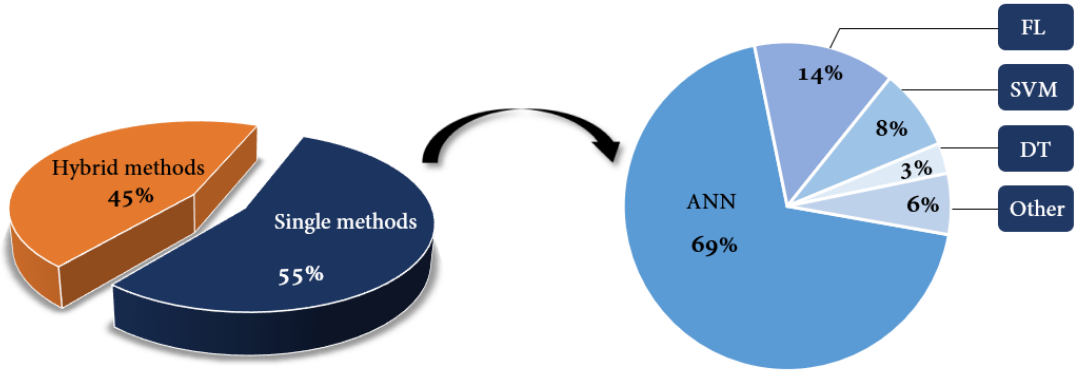

Fig. 6. Statistics of different AI method categories employed in the reviewed publications.

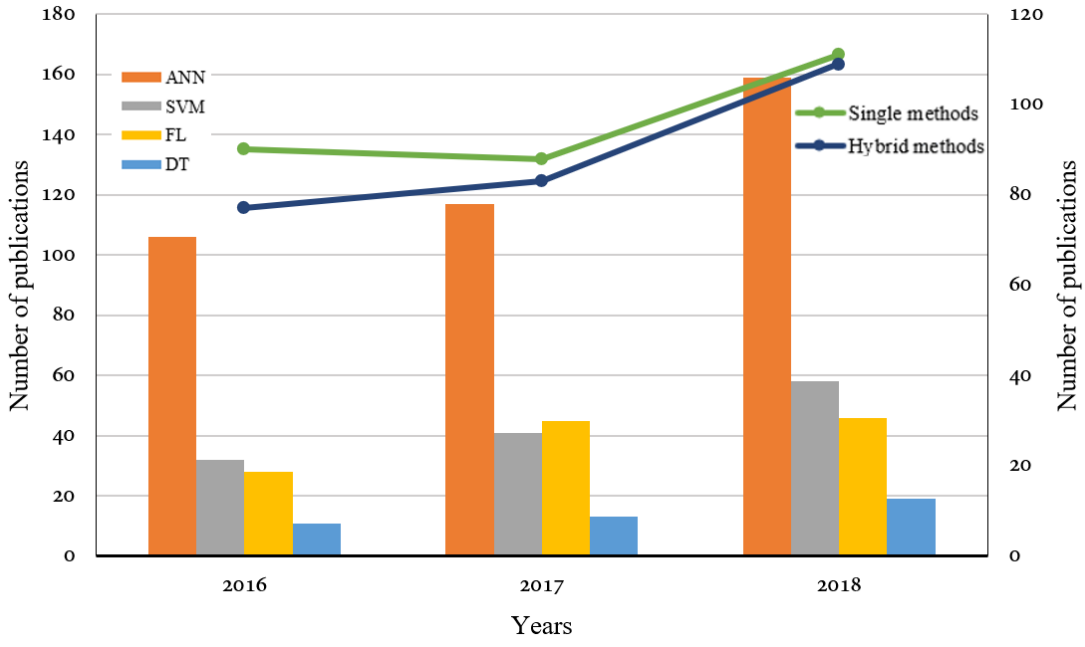

Fig. 7. Number of publications in the last three years, based on the ISI Web of Science.

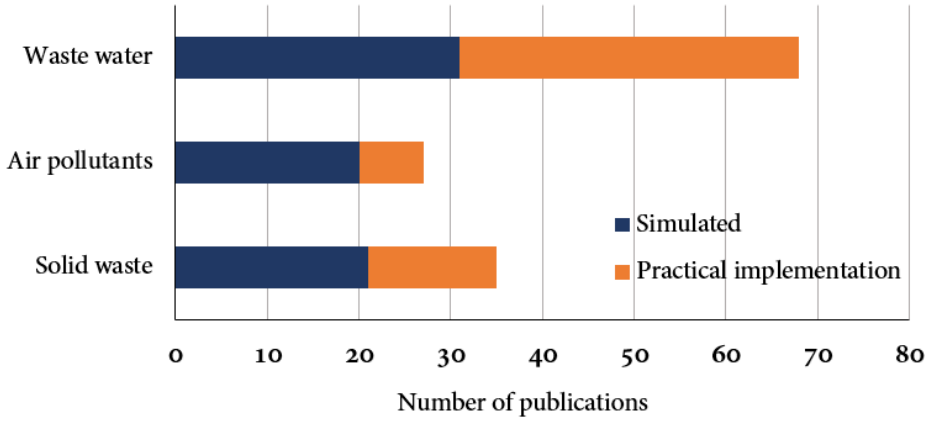

Fig. 8. Summary of applications of AI technologies for environmental pollution controls.

important influencing factors as well as model inputs. FL-based neuro-fuzzy systems, i.e. FNN and ANFIS, are the main technologies employed in intelligent control of aerobic stage of wastewater treatment process, the majority of the relevant works emphasized on cost-effective control of DO on-line for reducing total aeration time. AI soft-sensors are replacing traditional high-cost on-line instruments and off-line laboratorial analysis for estimation of hard-to-measure parameters in WWTPs, the on-line acquired pH, temperature and DO values were taken as necessary secondary variables to develop data-driven soft-sensors. At last, AI technologies especially hybrid AI methods has emerged as novel approaches for risk mapping and early-warning in both aquatic and atmospheric environments, they outperform existing statistical models in stability and accuracy.

As discussion and summary of the various AI applications shown in this review, the essential part for developing such a system is data that provides the connections between historical performance of the real system and a suitable model. The model is selected by testing different alternative AI models based on empirical experience for most of work, and the validation process is often performed by testing the historical data from real system. There is no doubt that AI technologies employed in this review are not completely summarized, but the samples of AI applications are enough to demonstrate the potential of AI technologies to tackle environmental challenges. Adaptive data-driven models with on-line learning abilities, which allow the models to directly use the real-time acquired information for training and adjusting structure and weights flexibility. Generally, it is hard to reach a standard to determine the AI technology for particular fields because of the diversities of application conditions and AI technologies. The existing

drawbacks of most AI models, which includes validation, computationally expensive, black-box, etc., should also be noted. To be more specific, sometimes the process of validation can be time-consuming to get an appropriate model. An AI model based on a small dataset may fail to achieve the desired accuracy, while the training process can be computationally expensive when it comes to a large dataset. As to the black-box nature, it will make models difficult to explicate the correlations between input and output variables. But the trend of using AI technologies to replace traditional mathematical methods is emerging due to the relatively reliable and rapid response, which should not be underestimated.

Acknowledgements

The authors are thanks for the National Natural Science Foundation of China (No. 51878614) and the financial support provided by Natural Science Foundation of ZheJiang Province (GB19041290088) for the financial support of this work.

1051 # Abbreviations

ABC	Artificial bee colony
AI	Artificial intelligence
AMODE	Adaptive multi-objective differential evolution
ANFIS	Adaptive network-based fuzzy inference system
ANN	Artificial neural network
AOPs	Advanced oxidation process
AQI	Air quality index
ASBWTP	Aerated submerged biofilm wastewater treatment process
ASP	Activated sludge process
AUC	Area under curve
BP	Back-propagation algorithm
BRT	Boosted regression tree
CART	Classification and regression tree
CEEMD-SVR-GWO	Complementary ensemble empirical mode decomposition hybrid with support vector regression and grey wolf optimizer
CEEMD-VMD-DE-ELM	Extreme learning machine hybrid with complementary ensemble empirical mode decomposition, variational mode decomposition and differential evolution algorithm
CNN	Convolutional neural network
CNN-LSTMNN	Convolutional neural network hybrid with long short-term memory neural network
DE	Differential evolution
DE-ANFIS	Differential evolution algorithm based adaptive neuro-fuzzy inference system
DT	Decision tree
EEMD	Ensemble empirical mode decomposition
EEMD-GRNN	Ensemble empirical mode decomposition based general regression neural network
ELM	Extreme learning machine
ELM-MARS-SVR-M5-ANN	Artificial neural network hybrid with extreme learning machines, multivariate regression splines, M5 Tree and support vector regression
ENN	Elman neural network
FL	Fuzzy logic
FL-SVM	Fuzzy logic based support vector machine
FNN	Fuzzy neural network
GA	Genetic algorithm
GA-ANFIS	Genetic algorithm based adaptive neuro-fuzzy inference system
GA-ANN	Genetic algorithm based artificial neural network
GA-FL-WNN	Wavelet neural network hybrid with genetic algorithm and fuzzy logic
GA-FNN	Genetic algorithm based fuzzy neural network
GA-GRNN	Genetic algorithm based general regression neural network
GA-SVR	Genetic algorithm based support vector regression

GBRT	Gradient boosting regression tree
GEP	Gene expression programming
GHG	Greenhouse gas
GRNN	General regression neural network
GWO	Grey wolf optimizer
IA	Immune algorithm
ICEEMDAN-ICA-ELM	Extreme learning machine hybrid with improved complete ensemble empirical mode decomposition with adaptive noise and imperialist competitive algorithm
ICS	Intelligent control system
kNN	k-nearest neighbor
LS-SVM	Least squares-support vector machine
LSTMNN	Long short-term memory neural network
MARS	Multi-adaptive regression spline
MBR	Membrane bio-reactor
MCSDE	Modified cuckoo search and differential evolution algorithm
MCSDE-CEEMD-ENN	Elman neural network hybrid with modified cuckoo search and differential evolution algorithm and complementary ensemble empirical mode decomposition
MLP	Multilayer perception
MLR	Multiple linear regression
MLR-ANN	Artificial neural network hybrid with multivariable linear regression
MSW	Municipal solid waste
OLS	Orthogonal least square
ORP	Oxidation-reduction potential
PAH	Polycyclic aromatic hydrocarbon
PCA	Principal component analysis
PCA-FNN	Principal component analysis based fuzzy neural network
PID	Proportion integration differentiation
PLS-RBFNN	Partial least square based radial basis function neural network
PLS-SVM	Partial least square based support vector machine
PMs	Particulate matters
PSO	Particle swarm optimization
PSO-ANN	Particle swarm optimization based artificial neural network
PSO-SDAE	Particle swarm optimization based stacked denoising auto-encoders deep network
RBF	Radial basis function
RBFNN	Radial basis function neural network
RF	Random forest
RMSE	Root mean square error
RNN	Recurrent neural network
RSM	Response surface methodology
RSM-ANN	Artificial neural network hybrid with response surface methodology
RSONN	Recurrent self-organizing neural network

RVM	Relevant vector machine
SBBR	Sequencing batch biofilm reactor process
SBR	Sequencing batch reactor activated sludge process
SCNN	Self-organizing cascade neural network
SDAE	Stacked denoising auto-encoders deep network
SDMINP	Simulation-based dynamic mixed integer nonlinear programming
SVD	Singular value decomposition
SVM	Support vector machine
SVR	Support vector regression
UASB	Upflow anaerobic sludge blanket reactor
VMD	Variational mode decomposition
VMD-CEEMDAN-ELM	Extreme learning machine hybrid with variational mode decomposition algorithm and complete ensemble empirical mode decomposition algorithm
WELLSVM	Weakly labeled support vector machine
WNN	Wavelet neural network
WWTPs	Wastewater treatment plants
ε-SVR	ε-support vector regression

1052
1053

References

Abbasi, M., Abduli, M.A., Omidvar, B., Baghvand, A., 2014. Results uncertainty of support vector machine and hybrid of wavelet transform-support vector machine models for solid waste generation forecasting. Environ. Prog. Sustain. Energy 33, 220–228. https://doi.org/10.1002/ep.11747

Abbasi, M., Abduli, M.A., Omidvar, B., Baghvand, A., 2013. Forecasting municipal solid waste generation by hybrid support vector machine and partial least square model. Int. J. Environ. Res. 7, 27–38.

Abbasi, M., El Hanandeh, A., 2016. Forecasting municipal solid waste generation using artificial intelligence modelling approaches. Waste Manag. 56, 13–22. https://doi.org/10.1016/j.wasman.2016.05.018

Abdoli, M.A., Nezhad, M.F., Sede, R.S., Behboudian, S., 2012. Longterm forecasting of solid waste generation by the artificial neural networks. Environ. Prog. Sustain. Energy 31, 628–636. https://doi.org/10.1002/ep.10591

Abiodun, O.I., Jantan, A., Omolara, A.E., Dada, K. V, Mohamed, N.A., Arshad, H., 2018. State-of-the-art in artificial neural network applications: A survey. Heliyon 4, e00938. https://doi.org/10.1016/j.heliyon.2018.e00938

Adamovic, V.M., Antanasijevic, D.Z., Cosovic, A.R., Ristic, M.D., Pocajt, V. V, 2018. An artificial neural network approach for the estimation of the primary production of energy from municipal solid waste and its application to the Balkan countries. Waste Manag. 78, 955–968. https://doi.org/10.1016/j.wasman.2018.07.012

Adamovic, V.M., Antanasijevic, D.Z., Ristic, M.A., Peric-Grujic, A.A., Pocajt, V. V, 2017. Prediction of municipal solid waste generation using artificial neural network approach enhanced by structural break analysis. Environ. Sci. Pollut. Res. 24, 299–311. https://doi.org/10.1007/s11356-016-7767-x

Adeyemi, A.S., Olorunfemi, J.F., Adewoye, T.O., 2001. Waste scavenging in Third World cities: A case study in Ilorin, Nigeria. Environmentalist, 21, 93–96. https://doi.org/10.1023/a:1010655623324

Agarwal, S., Tyagi, I., Gupta, V.K., Ghaedi, M., Masoomzade, M., Ghaedi, A.M., Mirtamizdoust, B., 2016. Kinetics and thermodynamics of methyl orange adsorption from aqueous solutions-artificial neural network-particle swarm optimization modeling. J. Mol. Liq. 218, 354–362. https://doi.org/10.1016/j.molliq.2016.02.048

Al-Obaidi, M.A., Li, J.P., Alsadaie, S., Kara-Zaïtri, C., Mujtaba, I.M., 2018. Modelling and optimisation of a multistage Reverse Osmosis processes with permeate reprocessing and recycling for the removal of N-nitrosodimethylamine from wastewater using Species Conserving Genetic Algorithms. Chem. Eng. J. 350, 824–834. https://doi.org/10.1016/j.cej.2018.06.022

Al-Obaidi, M.A., Li, J.P., Kara-Zaïtri, C., Mujtaba, I.M., 2017. Optimisation of reverse osmosis based wastewater treatment system for the removal of chlorophenol using genetic algorithms. Chem. Eng. J. 316, 91–100. https://doi.org/10.1016/j.cej.2016.12.096

Antanasijevic, D.Z., Pocajt, V. V, Povrenovic, D.S., Ristic, M.D., Peric-Grujic, A.A., 2013. PM_{10} emission forecasting using artificial neural networks and genetic algorithm input variable optimization. Sci. Total Environ. 443, 511–519. https://doi.org/10.1016/j.scitotenv.2012.10.110

Antwi, P., Li, J., Meng, J., Deng, K., Koblah Quashie, F., Li, J., Opoku Boadi, P., 2018. Feedforward

neural network model estimating pollutant removal process within mesophilic upflow anaerobic sludge blanket bioreactor treating industrial starch processing wastewater. Bioresour Technol 257, 102–112. https://doi.org/10.1016/j.biortech.2018.02.071

Arhami, M., Kamali, N., Rajabi, M.M., 2013. Predicting hourly air pollutant levels using artificial neural networks coupled with uncertainty analysis by Monte Carlo simulations. Environ. Sci. Pollut. Res. 20, 4777–4789. https://doi.org/10.1007/s11356-012-1451-6

Asadi, A., Verma, A., Yang, K., Mejabi, B., 2017. Wastewater treatment aeration process optimization: A data mining approach. J. Environ. Manage. 203, 630–639. https://doi.org/10.1016/j.jenvman.2016.07.047

Asfaram, A., Ghaedi, M., Ahmadi Azqhandi, M.H., Goudarzi, A., Hajati, S., 2017. Ultrasound-assisted binary adsorption of dyes onto Mn@ CuS/ZnS-NC-AC as a novel adsorbent: Application of chemometrics for optimization and modeling. J. Ind. Eng. Chem. 54, 377–388. https://doi.org/10.1016/j.jiec.2017.06.018

Asfaram, A., Ghaedi, M., Azqhandi, M.H.A., Goudarzi, A., Dastkhoon, M., 2016a. Statistical experimental design, least squares-support vector machine (LS-SVM) and artificial neural network (ANN) methods for modeling the facilitated adsorption of methylene blue dye. Rsc Adv. 6, 40502–40516. https://doi.org/10.1039/c6ra01874b

Asfaram, A., Ghaedi, M., Hajati, S., Goudarzi, A., 2016b. Synthesis of magnetic gamma-Fe_2O_3-based nanomaterial for ultrasonic assisted dyes adsorption: Modeling and optimization. Ultrason. Sonochem. 32, 418–431. https://doi.org/10.1016/j.ultsonch.2016.04.011

Assefi, P., Ghaedi, M., Ansari, A., Habibi, M.H., Momeni, M.S., 2014. Artificial neural network optimization for removal of hazardous dye Eosin Y from aqueous solution using Co_2O_3-NP-AC: Isotherm and kinetics study. J. Ind. Eng. Chem. 20, 2905–2913. https://doi.org/10.1016/j.jiec.2013.11.027

Azadi, S., Karimi-Jashni, A., 2016. Verifying the performance of artificial neural network and multiple linear regression in predicting the mean seasonal municipal solid waste generation rate: A case study of Fars province, Iran. Waste Manag. 48, 14–23. https://doi.org/10.1016/j.wasman.2015.09.034

Bagheri, A.R., Ghaedi, M., Asfaram, A., Hajati, S., Ghaedi, A.M., Bazrafshan, A., Rahimi, M.R., 2016. Modeling and optimization of simultaneous removal of ternary dyes onto copper sulfide nanoparticles loaded on activated carbon using second-derivative spectrophotometry. J. Taiwan Inst. Chem. Eng. 65, 212–224. https://doi.org/10.1016/j.jtice.2016.05.004

Bagheri, A.R., Ghaedi, M., Hajati, S., Ghaedi, A.M., Goudarzi, A., Asfaram, A., 2015. Random forest model for the ultrasonic-assisted removal of chrysoidine G by copper sulfide nanoparticles loaded on activated carbon; response surface methodology approach. Rsc Adv. 5, 59335–59343. https://doi.org/10.1039/c5ra08399k

Bagheri, M., Bazvand, A., Ehteshami, M., 2017. Application of artificial intelligence for the management of landfill leachate penetration into groundwater, and assessment of its environmental impacts. J. Clean. Prod. 149, 784–796. https://doi.org/10.1016/j.jclepro.2017.02.157

Bahrami, S., Niaei, A., Illán-Gómez, M.J., Tarjomannejad, A., Mousavi, S.M., Albaladejo-Fuentes, V., 2017. Catalytic reduction of NO by CO over CeO_2-MO_x (0.25) (M=Mn, Fe and Cu) mixed oxides—Modeling and optimization of catalyst preparation by hybrid ANN-GA. J. Environ. Chem. Eng. 5, 4937–4947. https://doi.org/https://doi.org/10.1016/j.jece.2017.09.023

Barzegar, R., Moghaddam, A.A., Deo, R., Fijani, E., Tziritis, E., 2018. Mapping groundwater contamination risk of multiple aquifers using multi-model ensemble of machine learning algorithms. Sci. Total Environ. 621, 697–712. https://doi.org/10.1016/j.scitotenv.2017.11.185

Beigl, P., Lebersorger, S., Salhofer, S., 2008. Modelling municipal solid waste generation: a review. Waste Manag 28, 200–214. https://doi.org/10.1016/j.wasman.2006.12.011

Biglarijoo, N., Mirbagheri, S.A., Bagheri, M., Ehteshami, M., 2017. Assessment of effective parameters in landfill leachate treatment and optimization of the process using neural network, genetic algorithm and response surface methodology. Process Saf. Environ. Prot. 106, 89–103. https://doi.org/10.1016/j.psep.2016.12.006

Bindal, S., Singh, C.K., 2019. Predicting groundwater arsenic contamination: Regions at risk in highest populated state of India. Water Res. 159, 65–76. https://doi.org/10.1016/j.watres.2019.04.054

Bui, D.T., Tsangaratos, P., Ngo, P.T.T., Pham, T.D., Pham, B.T., 2019. Flash flood susceptibility modeling using an optimized fuzzy rule based feature selection technique and tree based ensemble methods. Sci. Total Environ. 668, 1038–1054. https://doi.org/10.1016/j.scitotenv.2019.02.422

Bunsan, S., Chen, W.Y., Chen, H.W., Chuang, Y.H., Grisdanurak, N., 2013. Modeling the dioxin emission of a municipal solid waste incinerator using neural networks. Chemosphere 92, 258–264. https://doi.org/10.1016/j.chemosphere.2013.01.083

Buyukyildiz, M., Kumcu, S.Y., 2017. An estimation of the suspended sediment load using adaptive network based fuzzy inference system, support vector machine and artificial neural network models. Water Resour. Manag. 31, 1343–1359. https://doi.org/10.1007/s11269-017-1581-1

Buyukyildiz, M., Tezel, G., Yilmaz, V., 2014. Estimation of the change in lake water level by artificial intelligence methods. Water Resour. Manag. 28, 4747–4763. https://doi.org/10.1007/s11269-014-0773-1

Chambers, D.M., Reese, C.M., Thornburg, L.G., Sanchez, E., Rafson, J.P., Blount, B.C., Ruhl III, J.R.E., De Jesus, V.R., 2018. Distinguishing petroleum (crude oil and fuel) from smoke exposure within populations based on the relative blood levels of benzene, toluene, ethylbenzene, and xylenes (BTEX), styrene and 2,5-dimethylfuran by pattern recognition using artificial neural networks. Environ. Sci. Technol. 52, 308–316. https://doi.org/10.1021/acs.est.7b05128

Chang, F.J., Chung, C.H., Chen, P.A., Liu, C.W., Coynel, A., Vachaud, G., 2014. Assessment of arsenic concentration in stream water using neuro fuzzy networks with factor analysis. Sci. Total Environ. 494, 202–210. https://doi.org/10.1016/j.scitotenv.2014.06.133

Chang, N.B., Mohiuddin, G., Crawford, A.J., Bai, K.X., Jin, K.R., 2015. Diagnosis of the artificial intelligence-based predictions of flow regime in a constructed wetland for stormwater pollution control. Ecol. Inform. 28, 42–60. https://doi.org/10.1016/j.ecoinf.2015.05.001

Chen, J., Xie, C., Liu, J., He, Y., Xie, W., Zhang, X., Chang, K., Kuo, J., Sun, J., Zheng, L., Sun, S., Buyukada, M., Evrendilek, F., 2018. Co-combustion of sewage sludge and coffee grounds under increased O_2/CO_2 atmospheres: Thermodynamic characteristics, kinetics and artificial neural network modeling. Bioresour Technol 250, 230–238. https://doi.org/10.1016/j.biortech.2017.11.031

Chen, J.C., Liu, J.Y., He, Y., Huang, L.M., Sun, S.Y., Sun, J., Chang, K.L., Kuo, J.H., Huang, S.S., Ning, X.N., 2017. Investigation of co-combustion characteristics of sewage sludge and coffee grounds mixtures using thermogravimetric analysis coupled to artificial neural networks modeling. Bioresour. Technol. 225, 234–245. https://doi.org/10.1016/j.biortech.2016.11.069

Chen, K.Y., 2011. Combining linear and nonlinear model in forecasting tourism demand. Expert Syst. Appl. 38, 10368–10376. https://doi.org/10.1016/j.eswa.2011.02.049
Chen, W., Xie, X., Wang, J., Pradhan, B., Hong, H., Bui, D.T., Duan, Z., Ma, J., 2017. A comparative study of logistic model tree, random forest, and classification and regression tree models for spatial prediction of landslide susceptibility. Catena 151, 147–160. https://doi.org/10.1016/j.catena.2016.11.032
Chien-Cheng, L., Pau-Choo, C., Jea-Rong, T., Chein, I.C., 1999. Robust radial basis function neural networks. IEEE Trans. Syst. Man, Cybern. Part B 29, 674–685. https://doi.org/10.1109/3477.809023
Choubin, B., Darabi, H., Rahmati, O., Sajedi-Hosseini, F., Kløve, B., 2018. River suspended sediment modelling using the CART model: A comparative study of machine learning techniques. Sci. Total Environ. 615, 272–281. https://doi.org/10.1016/j.scitotenv.2017.09.293
Cong, Q.M., Yu, W., 2018. Integrated soft sensor with wavelet neural network and adaptive weighted fusion for water quality estimation in wastewater treatment process. Measurement 124, 436–446. https://doi.org/10.1016/j.measurement.2018.01.001
Costache, R., 2019. Flash-Flood Potential assessment in the upper and middle sector of Prahova river catchment (Romania). A comparative approach between four hybrid models. Sci. Total Environ. 659, 1115–1134. https://doi.org/10.1016/j.scitotenv.2018.12.397
Csábrági, A., Molnár, S., Tanos, P., Kovács, J., Molnár, M., Szabó, I., 2019. Estimation of dissolved oxygen in riverine ecosystems : Comparison of differently optimized neural networks. Ecol. Eng. 138, 298–309. https://doi.org/10.1016/j.ecoleng.2019.07.023
Dastkhoon, M., Ghaedi, M., Asfaram, A., Azqhandi, M.H.A., Purkait, M.K., 2017. Simultaneous removal of dyes onto nanowires adsorbent use of ultrasound assisted adsorption to clean waste water: Chemometrics for modeling and optimization, multicomponent adsorption and kinetic study. Chem. Eng. Res. Des. 124, 222–237. https://doi.org/10.1016/j.cherd.2017.06.011
Davis, L., 1991. Handbook of Genetic Algorithms, 1st ed. Van Nostrand Reinhold, New York.
Despagne, F., Massart, D.L., 1998. Neural networks in multivariate calibration. Analyst 123, 157–178.
Dieguez-Santana, K., Pham-The, H., Villegas-Aguilar, P.J., Le-Thi-Thu, H., Castillo-Garit, J.A., Casañola-Martin, G.M., 2016. Prediction of acute toxicity of phenol derivatives using multiple linear regression approach for Tetrahymena pyriformis contaminant identification in a median-size database. Chemosphere 165, 434–441. https://doi.org/https://doi.org/10.1016/j.chemosphere.2016.09.041
Dil, E.A., Ghaedi, M., Asfaram, A., Hajati, S., Mehrabi, F., Goudarzi, A., 2017. Preparation of nanomaterials for the ultrasound-enhanced removal of Pb^{2+} ions and malachite green dye: Chemometric optimization and modeling. Ultrason Sonochem 34, 677–691. https://doi.org/10.1016/j.ultsonch.2016.07.001
Dil, E.A., Ghaedi, M., Ghaedi, A., Asfaram, A., Jamshidi, M., Purkait, M.K., 2016. Application of artificial neural network and response surface methodology for the removal of crystal violet by zinc oxide nanorods loaded on activate carbon: kinetics and equilibrium study. J. Taiwan Inst. Chem. Eng. 59, 210–220. https://doi.org/10.1016/j.jtice.2015.07.023
Ding, D.H., Feng, C.P., Jin, Y.X., Hao, C.B., Zhao, Y.X., Suemura, T., 2011. Domestic sewage treatment in a sequencing batch biofilm reactor (SBBR) with an intelligent controlling system. Desalination 276, 260–265. https://doi.org/10.1016/j.desal.2011.03.059
Dolatabadi, M., Mehrabpour, M., Esfandyari, M., Alidadi, H., Davoudi, M., 2018. Modeling of

simultaneous adsorption of dye and metal ion by sawdust from aqueous solution using of ANN and ANFIS. Chemom. Intell. Lab. Syst. 181, 72–78. https://doi.org/10.1016/j.chemolab.2018.07.012

Eberhart, Yuhui, S., 2001. Particle swarm optimization: developments, applications and resources, in: Proceedings of the 2001 Congress on Evolutionary Computation. pp. 81–86. https://doi.org/10.1109/CEC.2001.934374

Esin, T., Cosgun, N., 2007. A study conducted to reduce construction waste generation in Turkey. Build. Environ. 42, 1667–1674. https://doi.org/10.1016/j.buildenv.2006.02.008

Fan, M., Hu, J., Cao, R., Ruan, W., Wei, X., 2018. A review on experimental design for pollutants removal in water treatment with the aid of artificial intelligence. Chemosphere 200, 330–343. https://doi.org/10.1016/j.chemosphere.2018.02.111

Fan, M.Y., Hu, J.W., Cao, R.S., Xiong, K.N., Wei, X.H., 2017. Modeling and prediction of copper removal from aqueous solutions by nZVI/rGO magnetic nanocomposites using ANN-GA and ANN-PSO. Sci. Rep. 7, 14. https://doi.org/10.1038/s41598-017-18223-y

Fernandez de Canete, J., Del Saz-Orozco, P., Baratti, R., Mulas, M., Ruano, A., Garcia-Cerezo, A., 2016. Soft-sensing estimation of plant effluent concentrations in a biological wastewater treatment plant using an optimal neural network. Expert Syst. Appl. 63, 8–19. https://doi.org/10.1016/j.eswa.2016.06.028

Fernández Núñez, E.G., Barchi, A.C., Ito, S., Escaramboni, B., Herculano, R.D., Roberta, C., Mayerd, M., Oliva Neto, P., 2017. Artificial intelligence approach for high level production of amylase using Rhizopus microsporus var. oligosporus and different agro-industrial wastes. J. Chem. Technol. Biotechnol. 92, 684–692. https://doi.org/10.1002/jctb.5054

Ferreira, A.R.L., Fernandes, L.F.S., Cortes, R.M. V, Pacheco, F.A.L., 2017. Science of the Total Environment Assessing anthropogenic impacts on riverine ecosystems using nested partial least squares regression. Sci. Total Environ. 583, 466–477. https://doi.org/10.1016/j.scitotenv.2017.01.106

Fijani, E., Barzegar, R., Deo, R., Tziritis, E., Konstantinos, S., 2019. Design and implementation of a hybrid model based on two-layer decomposition method coupled with extreme learning machines to support real-time environmental monitoring of water quality parameters. Sci. Total Environ. 648, 839–853. https://doi.org/10.1016/j.scitotenv.2018.08.221

Foscoliano, C., Del Vigo, S., Mulas, M., Tronci, S., 2016. Predictive control of an activated sludge process for long term operation. Chem. Eng. J. 304, 1031–1044. https://doi.org/10.1016/j.cej.2016.07.018

Gadekar, M.R., Ahammed, M.M., 2019. Modelling dye removal by adsorption onto water treatment residuals using combined response surface methodology-artificial neural network approach. J. Environ. Manage. 231, 241–248. https://doi.org/10.1016/j.jenvman.2018.10.017

Garcia Nieto, P.J., Garcia-Gonzalo, E., Alonso Fernandez, J.R., Diaz Muinz, C., 2019. Water eutrophication assessment relied on various machine learning techniques: A case study in the Englishmen Lake (Northern Spain). Ecol. Modell. 404, 91–102. https://doi.org/10.1016/j.ecolmodel.2019.03.009

Gaya, M.S., Wahab, N.A., Bature, A., Abubakar, U., Madugu, I.S., Kaurangini, M.L., Ila, L.B., 2015. Compensation control of dissolved oxygen in an activated sludge system via hybrid neuro fuzzy technique, in: Kurniawan, D., Nor, F.M. (Eds.), 2nd International Materials, Industrial, and Manufacturing Engineering Conference, Mimec2015. Elsevier Science Bv, Amsterdam, pp. 307–

312. https://doi.org/10.1016/j.promfg.2015.07.054
Genuino, D.A.D., Bataller, B.G., Capareda, S.C., de Luna, M.D.G., 2017. Application of artificial neural network in the modeling and optimization of humic acid extraction from municipal solid waste biochar. J. Environ. Chem. Eng. 5, 4101–4107. https://doi.org/10.1016/j.jece.2017.07.071
Geyikçi, F., Kılıç, E., Çoruh, S., Elevli, S., 2012. Modelling of lead adsorption from industrial sludge leachate on red mud by using RSM and ANN. Chem. Eng. J. 183, 53–59. https://doi.org/10.1016/j.cej.2011.12.019
Ghaedi, A.M., Ghaedi, M., Pouranfard, A.R., Ansari, A., Avazzadeh, Z., Vafaei, A., Tyagi, I., Agarwal, S., Gupta, V.K., 2016. Adsorption of Triamterene on multi-walled and single-walled carbon nanotubes: Artificial neural network modeling and genetic algorithm optimization. J. Mol. Liq. 216, 654–665. https://doi.org/10.1016/j.molliq.2016.01.068
Ghaedi, A.M., Vafaei, A., 2017. Applications of artificial neural networks for adsorption removal of dyes from aqueous solution: A review. Adv Colloid Interface Sci 245, 20–39. https://doi.org/10.1016/j.cis.2017.04.015
Ghaedi, M., Ansari, A., Bahari, F., Ghaedi, A.M., Vafaei, A., 2015. A hybrid artificial neural network and particle swarm optimization for prediction of removal of hazardous dye brilliant green from aqueous solution using zinc sulfide nanoparticle loaded on activated carbon. Spectrochim. Acta Part a-Molecular Biomol. Spectrosc. 137, 1004–1015. https://doi.org/10.1016/j.saa.2014.08.011
Ghaedi, M., Dashtian, K., Ghaedi, A.M., Dehghanian, N., 2016. A hybrid model of support vector regression with genetic algorithm for forecasting adsorption of malachite green onto multi-walled carbon nanotubes: central composite design optimization. Phys Chem Chem Phys 18, 13310–13321. https://doi.org/10.1039/c6cp01531j
Ghaedi, M., Ghaedi, A.M., Hossainpour, M., Ansari, A., Habibi, M.H., Asghari, A.R., 2014. Least square-support vector (LS-SVM) method for modeling of methylene blue dye adsorption using copper oxide loaded on activated carbon: Kinetic and isotherm study. J. Ind. Eng. Chem. 20, 1641–1649. https://doi.org/10.1016/j.jiec.2013.08.011
Goldberg, D.E., Holland, J.H., 1988. Genetic Algorithms and Machine Learning. Mach. Learn. 3, 95–99. https://doi.org/10.1023/a:1022602019183
Goonatilake, S., Khebbal, S., 1994. Intelligent Hybrid Systems, 1st ed. John Wiley & Sons, New York.
Gude, V.G., 2015. Energy and water autarky of wastewater treatment and power generation systems. Renew. Sustain. Energy Rev. 45, 52–68. https://doi.org/10.1016/j.rser.2015.01.055
Hadi, N., Niaei, A., Nabavi, S.R., Alizadeh, R., Shirazi, M.N., Izadkhand, B., 2016. An intelligent approach to design and optimization of M-Mn/H-ZSM-5 (M: Ce, Cr, Fe, Ni) catalysts in conversion of methanol to propylene. J. Taiwan Inst. Chem. Eng. 59, 173–185. https://doi.org/10.1016/j.jtice.2015.09.017
Haimi, H., Corona, F., Mulas, M., Sundell, L., Heinonen, M., Vahala, R., 2015. Shall we use hardware sensor measurements or soft-sensor estimates? Case study in a full-scale WWTP. Environ. Model. Softw. 72, 215–229. https://doi.org/10.1016/j.envsoft.2015.07.013
Haimi, H., Mulas, M., Corona, F., Vahala, R., 2013. Data-derived soft-sensors for biological wastewater treatment plants: An overview. Environ. Model. Softw. 47, 88–107. https://doi.org/10.1016/j.envsoft.2013.05.009
Han, H.G., Chen, Q.L., Qiao, J.F., 2011. An efficient self-organizing RBF neural network for water quality prediction. Neural Netw. 24, 717–725. https://doi.org/10.1016/j.neunet.2011.04.006
Han, H.G., Li, Y., Guo, Y.N., Qiao, J.F., 2016. A soft computing method to predict sludge volume

index based on a recurrent self-organizing neural network. Appl. Soft Comput. 38, 477–486. https://doi.org/10.1016/j.asoc.2015.09.051

Han, H.G., Zhu, S.G., Qiao, J.F., Guo, M., 2018. Data-driven intelligent monitoring system for key variables in wastewater treatment process. Chinese J. Chem. Eng. 26, 2093–2101. https://doi.org/10.1016/j.cjche.2018.03.027

Hazrati, H., Moghaddam, A.H., Rostamizadeh, M., 2017. The influence of hydraulic retention time on cake layer specifications in the membrane bioreactor: Experimental and artificial neural network modeling. J. Environ. Chem. Eng. 5, 3005–3013. https://doi.org/10.1016/j.jece.2017.05.050

He, J.J., Gong, S.L., Yu, Y., Yu, L.J., Wu, L., Mao, H.J., Song, C.B., Zhao, S.P., Liu, H.L., Li, X.Y., Li, R.P., 2017. Air pollution characteristics and their relation to meteorological conditions during 2014-2015 in major Chinese cities. Environ. Pollut. 223, 484–496. https://doi.org/10.1016/j.envpol.2017.01.050

He, J.J., Yu, Y., Xie, Y.C., Mao, H.J., Wu, L., Liu, N., Zhao, S.P., 2016. Numerical model-based artificial neural network model and its application for quantifying impact factors of urban air quality. Water Air Soil Pollut. 227, 16. https://doi.org/10.1007/s11270-016-2930-z

Hockett, D., Lober, D.J., Pilgrim, K., 1995. Determinants of per capita municipal solid waste generation in the southeastern united states. J. Environ. Manage. 45, 205–217. https://doi.org/10.1006/jema.1995.0069

Hong, H., Panahi, M., Shirzadi, A., Ma, T., Liu, J., Zhu, A.X., Chen, W., Kougias, I., Kazakis, N., 2018a. Flood susceptibility assessment in Hengfeng area coupling adaptive neuro-fuzzy inference system with genetic algorithm and differential evolution. Sci. Total Environ. 621, 1124–1141. https://doi.org/10.1016/j.scitotenv.2017.10.114

Hong, H., Tsangaratos, P., Ilia, I., Liu, J., Zhu, A.X., Chen, W., 2018b. Application of fuzzy weight of evidence and data mining techniques in construction of flood susceptibility map of Poyang County, China. Sci. Total Environ. 625, 575–588. https://doi.org/10.1016/j.scitotenv.2017.12.256

Hoseinian, F.S., Rezai, B., Kowsari, E., 2017. The nickel ion removal prediction model from aqueous solutions using a hybrid neural genetic algorithm. J. Environ. Manag. 204, 311–317. https://doi.org/10.1016/j.jenvman.2017.09.011

Huang, M.Z., Ma, Y.W., Wan, J.Q., Chen, X.H., 2015. A sensor-software based on a genetic algorithm-based neural fuzzy system for modeling and simulating a wastewater treatment process. Appl. Soft Comput. 27, 1–10. https://doi.org/10.1016/j.asoc.2014.10.034

Huang, M.Z., Ma, Y.W., Wan, J.Q., Wang, Y., Chen, Y.M., Yoo, C., 2014. Improving nitrogen removal using a fuzzy neural network-based control system in the anoxic/oxic process. Environ. Sci. Pollut. Res. 21, 12074–12084. https://doi.org/10.1007/s11356-014-3092-4

Huang, M.Z., Wan, J.Q., Ma, Y.W., Wang, Y., Li, W.J., Sun, X.F., 2009. Control rules of aeration in a submerged biofilm wastewater treatment process using fuzzy neural networks. Expert Syst. Appl. 36, 10428–10437. https://doi.org/10.1016/j.eswa.2009.01.035

Huang, Y.W., Chen, M.Q., 2015. Artificial neural network modeling of thin layer drying behavior of municipal sewage sludge. Measurement 73, 640–648. https://doi.org/10.1016/j.measurement.2015.06.014

Izadkhah, B., Nabavi, S.R., Niaei, A., Salari, D., Badiki, T.M., Caylak, N., 2012. Design and optimization of Bi-metallic Ag-ZSM5 catalysts for catalytic oxidation of volatile organic compounds. J. Ind. Eng. Chem. 18, 2083–2091. https://doi.org/10.1016/j.jiec.2012.06.002

Jaafari, A., Zenner, E.K., Panahi, M., Shahabi, H., 2019. Hybrid artificial intelligence models based on

a neuro-fuzzy system and metaheuristic optimization algorithms for spatial prediction of wildfire probability. Agric. For. Meteorol. 266–267, 198–207. https://doi.org/https://doi.org/10.1016/j.agrformet.2018.12.015

Jamshidi, M., Ghaedi, M., Dashtian, K., Ghaedi, A.M., Hajati, S., Goudarzi, A., Alipanahpour, E., 2016. Highly efficient simultaneous ultrasonic assisted adsorption of brilliant green and eosin B onto ZnS nanoparticles loaded activated carbon: Artificial neural network modeling and central composite design optimization. Spectrochim. Acta Part a-Molecular Biomol. Spectrosc. 153, 257–267. https://doi.org/10.1016/j.saa.2015.08.024

Jang, J.R., 1993. ANFIS: adaptive-network-based fuzzy inference system. IEEE Trans. Syst. Man. Cybern. 23, 665–685. https://doi.org/10.1109/21.256541

Jaramillo, F., Orchard, M., Muñoz, C., Antileo, C., Sáez, D., Espinoza, P., 2018. On-line estimation of the aerobic phase length for partial nitrification processes in SBR based on features extraction and SVM classification. Chem. Eng. J. 331, 114–123. https://doi.org/10.1016/j.cej.2017.07.185

Jing, L., Chen, B., Zhang, B.Y., 2014. Modeling of UV-induced photodegradation of naphthalene in marine oily wastewater by artificial neural networks. Water Air Soil Pollut. 225, 2–14. https://doi.org/10.1007/s11270-014-1906-0

Jing, L., Chen, B., Zhang, B.Y., Li, P., 2015. Process simulation and dynamic control for marine oily wastewater treatment using UV irradiation. Water Res. 81, 101–112. https://doi.org/10.1016/j.watres.2015.03.023

Johnson, N.E., Ianiuk, O., Cazap, D., Liu, L.L., Starobin, D., Dobler, G., Ghandehari, M., 2017. Patterns of waste generation: A gradient boosting model for short-term waste prediction in New York City. Waste Manag. 62, 3–11. https://doi.org/10.1016/j.wasman.2017.01.037

Kalogirou, S.A., 2003. Artificial intelligence for the modeling and control of combustion processes: a review. Prog. Energy Combust. Sci. 29, 515–566. https://doi.org/10.1016/s0360-1285(03)00058-3

Kamarul Zaman, N.A.F., Kanniah, K.D., Kaskaoutis, D.G., 2017. Estimating Particulate Matter using satellite based aerosol optical depth and meteorological variables in Malaysia. Atmos. Res. 193, 142–162. https://doi.org/10.1016/j.atmosres.2017.04.019

Kannangara, M., Dua, R., Ahmadi, L., Bensebaa, F., 2018. Modeling and prediction of regional municipal solid waste generation and diversion in Canada using machine learning approaches. Waste Manag. 74, 3–15. https://doi.org/10.1016/j.wasman.2017.11.057

Karimifard, S., Alavi Moghaddam, M.R., 2018. Application of response surface methodology in physicochemical removal of dyes from wastewater: A critical review. Sci. Total Environ. 640–641, 772–797. https://doi.org/10.1016/j.scitotenv.2018.05.355

Karri, R.R., Tanzifi, M., Yaraki, M.T., Sahu, J.N., 2018. Optimization and modeling of methyl orange adsorption onto polyaniline nano-adsorbent through response surface methodology and differential evolution embedded neural network. J. Environ. Manage. 223, 517–529. https://doi.org/10.1016/j.jenvman.2018.06.027

Kartic, D.N., Narayana, B.C.A., Arivazhagan, M., 2018. Removal of high concentration of sulfate from pigment industry effluent by chemical precipitation using barium chloride: RSM and ANN modeling approach. J. Environ. Manage. 206, 69–76. https://doi.org/10.1016/j.jenvman.2017.10.017

Kashiwao, T., Nakayama, K., Ando, S., Ikeda, K., Lee, M., Bahadori, A., 2017. A neural network-based local rainfall prediction system using meteorological data on the Internet: A case

study using data from the Japan Meteorological Agency. Appl. Soft Comput. 56, 317–330. https://doi.org/https://doi.org/10.1016/j.asoc.2017.03.015

Kasiri, M.B., Aleboyeh, H., Aleboyeh, A., 2008. Modeling and optimization of heterogeneous Photo-Fenton process with response surface methodology and artificial neural networks. Environ. Sci. Technol. 42, 7970–7975. https://doi.org/10.1021/es801372q

Khajeh, M., Kaykhaii, M., Sharafi, A., 2013. Application of PSO-artificial neural network and response surface methodology for removal of methylene blue using silver nanoparticles from water samples. J. Ind. Eng. Chem. 19, 1624–1630. https://doi.org/10.1016/j.jiec.2013.01.033

Khajeh, M., Sarafraz-Yazdi, A., Moghadam, A.F., 2017. Modeling of solid-phase tea waste extraction for the removal of manganese and cobalt from water samples by using PSO-artificial neural network and response surface methodology. Arab. J. Chem. 10, S1663–S1673. https://doi.org/10.1016/j.arabjc.2013.06.011

Khandanlou, R., Fard Masoumi, H.R., Ahmad, M.B., Shameli, K., Basri, M., Kalantari, K., 2016. Enhancement of heavy metals sorption via nanocomposites of rice straw and Fe 3 O 4 nanoparticles using artificial neural network (ANN). Ecol. Eng. 91, 249–256. https://doi.org/10.1016/j.ecoleng.2016.03.012

Khataee, A.R., Kasiri, M.B., 2010. Artificial neural networks modeling of contaminated water treatment processes by homogeneous and heterogeneous nanocatalysis. J. Mol. Catal. A-Chem. 331, 86–100. https://doi.org/10.1016/j.molcata.2010.07.016

Khosravi, K., Pham, B.T., Chapi, K., Shirzadi, A., Shahabi, H., Revhaug, I., Prakash, I., Tien Bui, D., 2018. A comparative assessment of decision trees algorithms for flash flood susceptibility modeling at Haraz watershed, northern Iran. Sci. Total Environ. 627, 744–755. https://doi.org/10.1016/j.scitotenv.2018.01.266

Kim, S., Pan, S., Mase, H., 2019. Artificial neural network-based storm surge forecast model: Practical application to Sakai Minato, Japan. Appl. Ocean Res. 91, 101871. https://doi.org/https://doi.org/10.1016/j.apor.2019.101871

Kontokosta, C.E., Hong, B., Johnson, N.E., Starobin, D., 2018. Using machine learning and small area estimation to predict building-level municipal solid waste generation in cities. Comput. Environ. Urban Syst. 70, 151–162. https://doi.org/10.1016/j.compenvurbsys.2018.03.004

Kumar, A., Samadder, S.R., 2017. An empirical model for prediction of household solid waste generation rate - A case study of Dhanbad, India. Waste Manag. 68, 3–15. https://doi.org/10.1016/j.wasman.2017.07.034

Kumar, A., Samadder, S.R., Kumar, N., Singh, C., 2018. Estimation of the generation rate of different types of plastic wastes and possible revenue recovery from informal recycling. Waste Manag. 79, 781–790. https://doi.org/10.1016/j.wasman.2018.08.045

Lek, S., Guegan, J.F., 1999. Artificial neural networks as a tool in ecological modelling, an introduction. Ecol. Modell. 120, 65–73. https://doi.org/10.1016/s0304-3800(99)00092-7

Leng, X.Z., Wang, J.H., Ji, H.B., Wang, Q.G., Li, H.M., Qian, X., Li, F.Y., Yang, M., 2017. Prediction of size-fractionated airborne particle-bound metals using MLR, BP-ANN and SVM analyses. Chemosphere 180, 513–522. https://doi.org/10.1016/j.chemosphere.2017.04.015

Lesnik, K.L., Liu, H., 2017. Predicting microbial fuel cell biofilm communities and bioreactor performance using artificial neural networks. Environ. Sci. Technol. 51, 10881–10892. https://doi.org/10.1021/acs.est.7b01413

Li, B., Yang, G., Wan, R., Hoermann, G., Huang, J., Fohrer, N., Zhang, L., 2017. Combining

multivariate statistical techniques and random forests model to assess and diagnose the trophic status of Poyang Lake in China. Ecol. Indic. 83, 74–83. https://doi.org/10.1016/j.ecolind.2017.07.033

Li, C., Sun, L., Jia, J., Cai, Y., Wang, X., 2016. Risk assessment of water pollution sources based on an integrated k-means clustering and set pair analysis method in the region of Shiyan, China. Sci. Total Environ. 557–558, 307–316. https://doi.org/10.1016/j.scitotenv.2016.03.069

Li, C., Zhu, Z.J., 2018. Research and application of a novel hybrid air quality early-warning system: A case study in China. Sci. Total Environ. 626, 1421–1438. https://doi.org/10.1016/j.scitotenv.2018.01.195

Li, F.J., Qiao, J.F., Han, H.G., Yang, C.L., 2016. A self-organizing cascade neural network with random weights for nonlinear system modeling. Appl. Soft Comput. 42, 184–193. https://doi.org/10.1016/j.asoc.2016.01.028

Lin, C.H., Yu, R.F., Cheng, W.P., Liu, C.R., 2012. Monitoring and control of UV and UV-TiO_2 disinfections for municipal wastewater reclamation using artificial neural networks. J. Hazard. Mater. 209, 348–354. https://doi.org/10.1016/j.jhazmat.2012.01.029

Lingamdinne, L.P., Singh, J., Choi, J.S., Chang, Y.Y., Yang, J.K., Karri, R.R., Koduru, J.R., 2018. Multivariate modeling via artificial neural network applied to enhance methylene blue sorption using graphene-like carbon material prepared from edible sugar. J. Mol. Liq. 265, 416–427. https://doi.org/10.1016/j.molliq.2018.06.022

Liu, L., Tang, Z., Kong, M., Chen, X., Zhou, C., Huang, K., Wang, Z., 2019. Tracing the potential pollution sources of the coastal water in Hong Kong with statistical models combining APCS-MLR. J. Environ. Manage. 245, 143–150. https://doi.org/10.1016/j.jenvman.2019.05.066

Liu, M., Lu, J., 2014. Support vector machine-an alternative to artificial neuron network for water quality forecasting in an agricultural nonpoint source polluted river? Environ. Sci. Pollut. Res. 21, 11036–11053. https://doi.org/10.1007/s11356-014-3046-x

Liu, Y.Q., Chen, J.D., Sun, Z.H., Li, Y., Huang, D.P., 2014. A probabilistic self-validating soft-sensor with application to wastewater treatment. Comput. Chem. Eng. 71, 263–280. https://doi.org/10.1016/j.compchemeng.2014.08.008

Longo, S., d'Antoni, B.M., Bongards, M., Chaparro, A., Cronrath, A., Fatone, F., Lema, J.M., Mauricio-Iglesias, M., Soares, A., Hospido, A., 2016. Monitoring and diagnosis of energy consumption in wastewater treatment plants. A state of the art and proposals for improvement. Appl. Energy 179, 1251–1268. https://doi.org/10.1016/j.apenergy.2016.07.043

Mahmoodi, N.M., Hosseinabadi-Farahani, Z., Chamani, H., 2016. Nanostructured adsorbent (MnO_2): Synthesis and least square support vector machine modeling of dye removal. Desalin. Water Treat. 57, 21524–21533. https://doi.org/10.1080/19443994.2015.1120685

Mandal, S., Mahapatra, S.S., Sahu, M.K., Patel, R.K., 2015. Artificial neural network modelling of As(III) removal from water by novel hybrid material. Process Saf. Environ. Prot. 93, 249–264. https://doi.org/10.1016/j.psep.2014.02.016

Mazaheri, H., Ghaedi, M., Azqhandi, M.H.A., Asfaram, A., 2017. Application of machine/statistical learning, artificial intelligence and statistical experimental design for the modeling and optimization of methylene blue and Cd(II) removal from a binary aqueous solution by natural walnut carbon. Phys. Chem. Chem. Phys. 19, 11299–11317. https://doi.org/10.1039/c6cp08437k

McCulloch, W.S., Pitts, W., 1943. A logical calculus of the ideas immanent in nervous activity. Bull Math Biophys 5, 115–133. https://doi.org/10.1007/bf02478259

Medsker, L.R., 1995. Hybrid Intelligent Systems, 1st ed. Kluwer Academic Publishers, New York.
Messikh, N., Chiha, M., Ahmedchekkat, F., Al Bsoul, A., 2015. Application of radial basis function neural network for removal of copper using an emulsion liquid membrane process assisted by ultrasound. Desalin. Water Treat. 56, 399–408. https://doi.org/10.1080/19443994.2014.936513
Mohd Ali, J., Hussain, M.A., Tade, M.O., Zhang, J., 2015. Artificial Intelligence techniques applied as estimator in chemical process systems - A literature survey. Expert Syst. Appl. 42, 5915–5931. https://doi.org/10.1016/j.eswa.2015.03.023
Moosavi, M., Soltani, N., 2013. Prediction of hydrocarbon densities using an artificial neural network-group contribution method up to high temperatures and pressures. Thermochim. Acta 556, 89–96. https://doi.org/10.1016/j.tca.2013.01.038
Mulas, M., Corona, F., Haimi, H., Sundell, L., Heinonen, M., Vahala, R., 2011. Estimating nitrate concentration in the post-denitrification unit of a municipal wastewater treatment plant. IFAC Proc. Vol. 44, 6212–6217. https://doi.org/https://doi.org/10.3182/20110828-6-IT-1002.02931
Nabavi-Pelesaraei, A., Bayat, R., Hosseinzadeh-Bandbafha, H., Afrasyabi, H., Berrada, A., 2017. Prognostication of energy use and environmental impacts for recycle system of municipal solid waste management. J. Clean. Prod. 154, 602–613. https://doi.org/10.1016/j.jclepro.2017.04.033
Nabavi-Pelesaraei, A., Rafiee, S., Mohtasebi, S.S., Hosseinzadeh-Bandbafha, H., Chau, K. wing, 2018. Integration of artificial intelligence methods and life cycle assessment to predict energy output and environmental impacts of paddy production. Sci. Total Environ. 631–632, 1279–1294. https://doi.org/10.1016/j.scitotenv.2018.03.088
Nadiri, A.A., Shokri, S., Tsai, F.T.C., Moghaddam, A.A., 2018. Prediction of effluent quality parameters of a wastewater treatment plant using a supervised committee fuzzy logic model. J. Clean. Prod. 180, 539–549. https://doi.org/10.1016/j.jclepro.2018.01.139
Nag, S., Mondal, A., Roy, D.N., Bar, N., Das, S.K., 2018. Sustainable bioremediation of Cd(II) from aqueous solution using natural waste materials: Kinetics, equilibrium, thermodynamics, toxicity studies and GA-ANN hybrid modelling. Environ. Technol. Innov. 11, 83–104. https://doi.org/10.1016/j.eti.2018.04.009
Nandagopal, M.S.G., Abraham, E., Selvaraju, N., 2017. Advanced neural network prediction and system identification of liquid-liquid flow patterns in circular microchannels with varying angle of confluence. Chem. Eng. J. 309, 850–865. https://doi.org/10.1016/j.cej.2016.10.106
Niaei, A., Badiki, T.M., Nabavi, S.R., Salari, D., Izadkhah, B., Caylak, N., 2013. Neuro-genetic aided design of modified H-ZSM-5 catalyst for catalytic conversion of methanol to gasoline range hydrocarbons. J. Taiwan Inst. Chem. Eng. 44, 247–256. https://doi.org/10.1016/j.jtice.2012.11.008
Niu, M.F., Wang, Y.F., Sun, S.L., Li, Y.W., 2016. A novel hybrid decomposition-and-ensemble model based on CEEMD and GWO for short-term $PM_{2.5}$ concentration forecasting. Atmos. Environ. 134, 168–180. https://doi.org/10.1016/j.atmosenv.2016.03.056
Noori, R., Abdoli, M., Ghazizade, M.J., Samieifard, R., 2009. Comparison of neural network and principal component-regression analysis to predict the solid waste generation in Tehran. Iran J. Public Heal. 38, 74–84.
Noori, R., Karbassi, A., Salman Sabahi, M., 2010. Evaluation of PCA and Gamma test techniques on ANN operation for weekly solid waste prediction. J Env. Manag. 91, 767–771. https://doi.org/10.1016/j.jenvman.2009.10.007
Nourani, V., Molajou, A., Tajbakhsh, A.D., Najafi, H., 2019. A wavelet based data mining technique

for suspended sediment load modeling. Water Resour. Manag. 33, 1769–1784. https://doi.org/10.1007/s11269-019-02216-9

Offenberg, J.H., Lewandowski, M., Kleindienst, T.E., Docherty, K.S., Jaoui, M., Krug, J., Riedel, T.P., Olson, D.A., 2017. Predicting thermal behavior of secondary organic aerosols. Environ. Sci. Technol. 51, 9911–9919. https://doi.org/10.1021/acs.est.7b01968

Oliveira, V., Sousa, V., Dias-Ferreira, C., 2019. Artificial neural network modelling of the amount of separately-collected household packaging waste. J. Clean. Prod. 210, 401–409. https://doi.org/10.1016/j.jclepro.2018.11.063

Olsson, G., 2012. ICA and me - A subjective review. Water Res. 46, 1585–1624. https://doi.org/10.1016/j.watres.2011.12.054

Pai, P.-F., Lin, K.-P., Lin, C.-S., Chang, P.-T., 2010. Time series forecasting by a seasonal support vector regression model. Expert Syst. Appl. 37, 4261–4265. https://doi.org/https://doi.org/10.1016/j.eswa.2009.11.076

Pai, T.Y., Yang, P.Y., Wang, S.C., Lo, M.H., Chiang, C.F., Kuo, J.L., Chu, H.H., Su, H.C., Yu, L.F., Hu, H.C., Chang, Y.H., 2011. Predicting effluent from the wastewater treatment plant of industrial park based on fuzzy network and influent quality. Appl. Math. Model. 35, 3674–3684. https://doi.org/10.1016/j.apm.2011.01.019

Pandey, D.S., Das, S., Pan, I., Leahy, J.J., Kwapinski, W., 2016. Artificial neural network based modelling approach for municipal solid waste gasification in a fluidized bed reactor. Waste Manag. 58, 202–213. https://doi.org/10.1016/j.wasman.2016.08.023

Park, J., Sandberg, I.W., 1991. Universal approximation using radial-basis-function networks. Neural Comput. 3, 246–257. https://doi.org/10.1162/neco.1991.3.2.246

Park, S., Kim, M., Kim, M., Namgung, H.G., Kim, K.T., Cho, K.H., Kwon, S.B., 2018. Predicting PM_{10} concentration in Seoul metropolitan subway stations using artificial neural network (ANN). J. Hazard. Mater. 341, 75–82. https://doi.org/10.1016/j.jhazmat.2017.07.050

Pearce, A.R., Rizzo, D.M., Watzin, M.C., Druschel, G.K., 2013. Unraveling associations between cyanobacteria blooms and in-lake environmental conditions in Missisquoi Bay, Lake Champlain, USA, using a modified self-organizing map. Environ. Sci. Technol. 47, 14267–14274. https://doi.org/10.1021/es403490g

Qiao, J.F., Hou, Y., Zhang, L., Han, H.G., 2018. Adaptive fuzzy neural network control of wastewater treatment process with multiobjective operation. Neurocomputing 275, 383–393. https://doi.org/10.1016/j.neucom.2017.08.059

Rego, A.S.C., Valim, I.C., Vieira, A.A.S., Vilani, C., Santos, B.F., 2018. Optimization of sugarcane bagasse pretreatment using alkaline hydrogen peroxide through ANN and ANFIS modelling. Bioresour. Technol. 267, 634–641. https://doi.org/10.1016/j.biortech.2018.07.087

Rocha, S.J.S.S. da, Torres, C.M.M.E., Jacovine, L.A.G., Leite, H.G., Gelcer, E.M., Neves, K.M., Schettini, B.L.S., Villanova, P.H., Silva, L.F. da, Reis, L.P., Zanuncio, J.C., 2018. Artificial neural networks: Modeling tree survival and mortality in the Atlantic Forest biome in Brazil. Sci. Total Environ. 645, 655–661. https://doi.org/10.1016/j.scitotenv.2018.07.123

Ruan, J.J., Zhang, C., Li, Y., Li, P.Y., Yang, Z.Z., Chen, X.H., Huang, M.Z., Zhang, T., 2017. Improving the efficiency of dissolved oxygen control using an on-line control system based on a genetic algorithm evolving FWNN software sensor. J. Environ. Manage. 187, 550–559. https://doi.org/10.1016/j.jenvman.2016.10.056

Sabour, M.R., Amiri, A., 2017. Comparative study of ANN and RSM for simultaneous optimization of

multiple targets in Fenton treatment of landfill leachate. Waste Manag. 65, 54–62. https://doi.org/10.1016/j.wasman.2017.03.048
Salehi, I., Shirani, M., Semnani, A., Hassani, M., Habibollahi, S., 2016. Comparative study between response surface methodology and artificial neural network for adsorption of crystal violet on magnetic activated carbon. Arab. J. Sci. Eng. 41, 2611–2621. https://doi.org/10.1007/s13369-016-2109-3
Santin, I., Barbu, M., Pedret, C., Vilanova, R., 2018. Fuzzy logic for plant-wide control of biological wastewater treatment process including greenhouse gas emissions. Isa Trans. 77, 146–166. https://doi.org/10.1016/j.isatra.2018.04.006
Sarigiannis, D.A., Karakitsios, S.P., Kermenidou, M., Nikolaki, S., Zikopoulos, D., Semelidis, S., Papagiannakis, A., Tzimou, R., 2014. Total exposure to airborne particulate matter in cities: The effect of biomass combustion. Sci. Total Environ. 493, 795–805. https://doi.org/10.1016/j.scitotenv.2014.06.055
Scholkopf, B., Smola, A.J., 2001. Learning with Kernels: Support Vector Machines, Regularization, Optimization, and Beyond, 1st ed. MIT Press, Cambridge.
Selvakumar, P., Sivashanmugam, P., 2018. Multi-hydrolytic biocatalyst from organic solid waste and its application in municipal waste activated sludge pre-treatment towards energy recovery. Process Saf. Environ. Prot. 117, 1–10. https://doi.org/10.1016/j.psep.2018.03.036
Sha'Ato, R., Aboho, S.Y., Oketunde, F.O., Eneji, I.S., Unazi, G., Agwa, S., 2007. Survey of solid waste generation and composition in a rapidly growing urban area in Central Nigeria. Waste Manag. 27, 352–358. https://doi.org/10.1016/j.wasman.2006.02.008
Shamiri, A., Wong, S.W., Zanil, M.F., Hussain, M.A., Mostoufi, N., 2015. Modified two-phase model with hybrid control for gas phase propylene copolymerization in fluidized bed reactors. Chem. Eng. J. 264, 706–719. https://doi.org/10.1016/j.cej.2014.11.104
Shang, Z., Deng, T., He, J., Duan, X., 2019. A novel model for hourly $PM_{2.5}$ concentration prediction based on CART and EELM. Sci. Total Environ. 651, 3043–3052. https://doi.org/10.1016/j.scitotenv.2018.10.193
Sharghi, E., Nourani, V., Najafi, H., Gokcekus, H., 2019. Conjunction of a newly proposed emotional ANN (EANN) and wavelet transform for suspended sediment load modeling. Water Sci. Technol.-Water Supply 19, 1726–1734. https://doi.org/10.2166/ws.2019.044
Shen, W., Tao, E., Chen, X., Liu, D., Liu, H., 2014. Nitrate control strategies in an activated sludge wastewater treatment process. Korean J. Chem. Eng. 31, 386–392. https://doi.org/10.1007/s11814-013-0237-y
Shi, B., Wang, P., Jiang, J., Liu, R., 2018. Applying high-frequency surrogate measurements and a wavelet-ANN model to provide early warnings of rapid surface water quality anomalies. Sci. Total Environ. 610–611, 1390–1399. https://doi.org/10.1016/j.scitotenv.2017.08.232
Shi, S., Xu, G., 2018. Novel performance prediction model of a biofilm system treating domestic wastewater based on stacked denoising auto-encoders deep learning network. Chem. Eng. J. 347, 280–290. https://doi.org/10.1016/j.cej.2018.04.087
Shi, Y., Eberhart, R., 1998. A modified particle swarm optimizer, in: 1998 IEEE International Conference on Evolutionary Computation Proceedings. IEEE World Congress on Computational Intelligence. pp. 69–73. https://doi.org/10.1109/ICEC.1998.699146
Shokry, A., Vicente, P., Escudero, G., Pérez-Moya, M., Graells, M., Espuña, A., 2018. Data-driven soft-sensors for online monitoring of batch processes with different initial conditions. Comput.

Chem. Eng. 118, 159–179. https://doi.org/https://doi.org/10.1016/j.compchemeng.2018.07.014
Singh, K.P., Gupta, S., Kumar, A., Shukla, S.P., 2012. Linear and nonlinear modeling approaches for urban air quality prediction. Sci. Total Environ. 426, 244–255. https://doi.org/10.1016/j.scitotenv.2012.03.076
Singh, K.P., Gupta, S., Ojha, P., Rai, P., 2013. Predicting adsorptive removal of chlorophenol from aqueous solution using artificial intelligence based modeling approaches. Env. Sci Pollut Res Int 20, 2271–2287. https://doi.org/10.1007/s11356-012-1102-y
Soleymani, A.R., Moradi, M., 2018. Performance and modeling of UV/persulfate/Ce(IV) process as a dual oxidant photochemical treatment system: Kinetic study and operating cost estimation. Chem. Eng. J. 347, 243–251. https://doi.org/10.1016/j.cej.2018.04.093
Strnad, D., Guid, N., 2010. A fuzzy-genetic decision support system for project team formation. Appl. Soft Comput. 10, 1178–1187. https://doi.org/10.1016/j.asoc.2009.08.032
Suárez-escobar, A., Pataquiva-mateus, A., López-vasquez, A., 2016. Electrocoagulation-photocatalytic process for the treatment of lithographic wastewater . Optimization using response surface methodology (RSM) and kinetic study. Catal. Today 266, 120–125. https://doi.org/10.1016/j.cattod.2015.09.016
Sun, N., Chungpaibulpatana, S., 2017. Development of an Appropriate Model for Forecasting Municipal Solid Waste Generation in Bangkok, in: Waewsak, J., Sangkharak, K., Othong, S., Gagnon, Y. (Eds.), 2017 International Conference on Alternative Energy in Developing Countries and Emerging Economies. Elsevier Science Bv, Amsterdam, pp. 907–912. https://doi.org/10.1016/j.egypro.2017.10.134
Sun, S.C., Bao, Z.Y., Li, R.Y., Sun, D.Z., Geng, H.H., Huang, X.F., Lin, J.H., Zhang, P.X., Ma, R., Fang, L., Zhang, X.H., Zhao, X.X., 2017. Reduction and prediction of N_2O emission from an Anoxic/Oxic wastewater treatment plant upon DO control and model simulation. Bioresour. Technol. 244, 800–809. https://doi.org/10.1016/j.biortech.2017.08.054
Suykens, J.A.K., Vandewalle, J., 1999. Least squares support vector machine classifiers. Neural Process. Lett. 9, 293–300. https://doi.org/10.1023/a:1018628609742
Taghvaei, H., Amooie, M.A., Hemmati-Sarapardeh, A., Taghvaei, H., 2016. A comprehensive study of phase equilibria in binary mixtures of carbon dioxide plus alcohols: Application of a hybrid intelligent model (CSA-LSSVM). J. Mol. Liq. 224, 745–756. https://doi.org/10.1016/j.molliq.2016.09.119
Tan, K.C., Lim, H.S., Zubir, M., Jafri, M., 2016. Prediction of column ozone concentrations using multiple regression analysis and principal component analysis techniques : A case study in peninsular Malaysia. Atmos. Pollut. Res. 7, 533–546. https://doi.org/10.1016/j.apr.2016.01.002
Tanhaei, B., Ayati, A., Lahtinen, M., Vaziri, B.M., Sillanpaa, M., 2016. A magnetic mesoporous chitosan based core-shells biopolymer for anionic dye adsorption: Kinetic and isothermal study and application of ANN. J. Appl. Polym. Sci. 133, 11. https://doi.org/10.1002/app.43466
Tatar, A., Naseri, S., Bahadori, M., Hezave, A.Z., Kashiwao, T., Bahadori, A., Darvish, H., 2016. Prediction of carbon dioxide solubility in ionic liquids using MLP and radial basis function (RBF) neural networks. J. Taiwan Inst. Chem. Eng. 60, 151–164. https://doi.org/10.1016/j.jtice.2015.11.002
Thoe, W., Wong, S.H.C., Choi, K.W., Lee, J.H.W., 2012. Daily prediction of marine beach water quality in Hong Kong. J. Hydro-Environment Res. 6, 164–180. https://doi.org/10.1016/j.jher.2012.05.003

Tiwari, M.K., Bajpai, S., 2012. Prediction of industrial solid waste with ANFIS model and its comparison with ANN model-A case study of Durg-Bhilai twin city India. Int. J. Eng. Innov. Technol. 6, 192–201.

Turan, N.G., Mesci, B., Ozgonenel, O., 2011. The use of artificial neural networks (ANN) for modeling of adsorption of Cu(II) from industrial leachate by pumice. Chem. Eng. J. 171, 1091–1097. https://doi.org/10.1016/j.cej.2011.05.005

Vani, S., Sukumaran, R.K., Savithri, S., 2015. Prediction of sugar yields during hydrolysis of lignocellulosic biomass using artificial neural network modeling. Bioresour. Technol. 188, 128–135. https://doi.org/10.1016/j.biortech.2015.01.083

Vapnik, V.N., 1995. The Nature of Statistical Learning Theory. Springer, New York.

Voukantsis, D., Karatzas, K., Kukkonen, J., Rasanen, T., Karppinen, A., Kolehmainen, M., 2011. Intercomparison of air quality data using principal component analysis, and forecasting of PM_{10} and $PM_{2.5}$ concentrations using artificial neural networks, in Thessaloniki and Helsinki. Sci. Total Environ. 409, 1266–1276. https://doi.org/10.1016/j.scitotenv.2010.12.039

Wan, J.Q., Huang, M.Z., Ma, Y.W., Guo, W.J., Wang, Y., Zhang, H.P., Li, W.J., Sun, X.F., 2011. Prediction of effluent quality of a paper mill wastewater treatment using an adaptive network-based fuzzy inference system. Appl. Soft Comput. 11, 3238–3246. https://doi.org/10.1016/j.asoc.2010.12.026

Wang, C., Ye, Z., Yu, Y., Gong, W., 2018. Estimation of bus emission models for different fuel types of buses under real conditions. Sci. Total Environ. 640–641, 965–972. https://doi.org/10.1016/j.scitotenv.2018.05.289

Wang, D., Wei, S., Luo, H., Yue, C., Grunder, O., 2017. A novel hybrid model for air quality index forecasting based on two-phase decomposition technique and modified extreme learning machine. Sci. Total Environ. 580, 719–733. https://doi.org/10.1016/j.scitotenv.2016.12.018

Wang, P., Liu, Y., Qin, Z.D., Zhang, G.S., 2015. A novel hybrid forecasting model for PM_{10} and SO_2 daily concentrations. Sci. Total Environ. 505, 1202–1212. https://doi.org/10.1016/j.scitotenv.2014.10.078

Wei, L., Hu, Z., Dong, L., Zhao, W., 2015. A damage assessment model of oil spill accident combining historical data and satellite remote sensing information: A case study in Penglai 19-3 oil spill accident of China. Mar. Pollut. Bull. 91, 258–271. https://doi.org/10.1016/j.marpolbul.2014.11.036

Wen, C.C., Liu, S., Yao, X.J., Peng, L., Li, X., Hu, Y., Chi, T.H., 2019. A novel spatiotemporal convolutional long short-term neural network for air pollution prediction. Sci. Total Environ. 654, 1091–1099. https://doi.org/10.1016/j.scitotenv.2018.11.086

Wen, X., Gong, B.Z., Zhou, J., He, Q., Qing, X.X., 2017. Efficient simultaneous partial nitrification, anammox and denitrification (SNAD) system equipped with a real-time dissolved oxygen (DO) intelligent control system and microbial community shifts of different substrate concentrations. Water Res. 119, 201–211. https://doi.org/10.1016/j.watres.2017.04.052

Xie, C.D., Liu, J.Y., Zhang, X.C., Xie, W.M., Sun, J., Chang, K.L., Kuo, J.H., Xie, W.H., Liu, C., Sun, S.Y., Buyukada, M., Evrendilek, F., 2018. Co-combustion thermal conversion characteristics of textile dyeing sludge and pomelo peel using TGA and artificial neural networks. Appl. Energy 212, 786–795. https://doi.org/10.1016/j.apenergy.2017.12.084

Xu, G., Yu, G.S., 2018. Reprint of: On convergence analysis of particle swarm optimization algorithm. J. Comput. Appl. Math. 340, 709–717. https://doi.org/10.1016/j.cam.2018.04.036

Yang, Z.S., Wang, J., 2017. A new air quality monitoring and early warning system: Air quality assessment and air pollutant concentration prediction. Environ. Res. 158, 105–117. https://doi.org/10.1016/j.envres.2017.06.002

Yasin, Y., Ahmad, F.B.H., Ghaffari-Moghaddam, M., Khajeh, M., 2014. Application of a hybrid artificial neural network–genetic algorithm approach to optimize the lead ions removal from aqueous solutions using intercalated tartrate-Mg–Al layered double hydroxides. Environ. Nanotechnol. Monit. Manag. 1–2, 2–7. https://doi.org/10.1016/j.enmm.2014.03.001

Ye, L., Gao, L., Marcos-Martinez, R., Mallants, D., Bryan, B.A., 2019. Projecting Australia's forest cover dynamics and exploring influential factors using deep learning. Environ. Model. Softw. 119, 407–417. https://doi.org/https://doi.org/10.1016/j.envsoft.2019.07.013

Yilmaz, B., Aras, E., Nacar, S., Kankal, M., 2018. Estimating suspended sediment load with multivariate adaptive regression spline, teaching-learning based optimization, and artificial bee colony models. Sci. Total Environ. 639, 826–840. https://doi.org/10.1016/j.scitotenv.2018.05.153

Yilmaz, I., Kaynar, O., 2011. Multiple regression, ANN (RBF, MLP) and ANFIS models for prediction of swell potential of clayey soils. Expert Syst. Appl. 38, 5958–5966. https://doi.org/https://doi.org/10.1016/j.eswa.2010.11.027

Yoo, K., Shukla, S.K., Ahn, J.J., Oh, K., Park, J., 2016. Decision tree-based data mining and rule induction for identifying hydrogeological parameters that influence groundwater pollution sensitivity. J. Clean. Prod. 122, 277–286. https://doi.org/10.1016/j.jclepro.2016.01.075

You, Z., Zhu, Y., Jang, C., Wang, S., Gao, J., Lin, C., Li, M., Zhu, Z., Wei, H., Yang, W., 2016. Response surface modeling-based source contribution analysis and VOC emission control policy assessment in a typical ozone-polluted urban Shunde, China. J. Environ. Sci. 51, 294–304. https://doi.org/10.1016/j.jes.2016.05.034

Yu, R.-F., Chi, F.-H., Cheng, W.-P., Chang, J.-C., 2014. Application of pH, ORP, and DO monitoring to evaluate chromium(VI) removal from wastewater by the nanoscale zero-valent iron (nZVI) process. Chem. Eng. J. 255, 568–576. https://doi.org/10.1016/j.cej.2014.06.002

Yu, R.-F., Lin, C.-H., Chen, H.-W., Cheng, W.-P., Kao, M.-C., 2013. Possible control approaches of the Electro-Fenton process for textile wastewater treatment using on-line monitoring of DO and ORP. Chem. Eng. J. 218, 341–349. https://doi.org/10.1016/j.cej.2012.12.061

Zhang, B., Yang, C., Zhu, H., Li, Y., Gui, W., 2016. Evaluation strategy for the control of the copper removal process based on oxidation–reduction potential. Chem. Eng. J. 284, 294–304. https://doi.org/10.1016/j.cej.2015.07.094

Zhang, H., Wu, P., Yin, A., Yang, X., Zhang, M., Gao, C., 2017. Prediction of soil organic carbon in an intensively managed reclamation zone of eastern China: A comparison of multiple linear regressions and the random forest model. Sci. Total Environ. 592, 704–713. https://doi.org/10.1016/j.scitotenv.2017.02.146

Zhang, R., Chen, Z.Y., Xu, L.J., Ou, C.Q., 2019. Meteorological drought forecasting based on a statistical model with machine learning techniques in Shaanxi province, China. Sci. Total Environ. 665, 338–346. https://doi.org/10.1016/j.scitotenv.2019.01.431

Zhang, Y., Pan, B., 2014. Modeling batch and column phosphate removal by hydrated ferric oxide-based nanocomposite using response surface methodology and artificial neural network. Chem. Eng. J. 249, 111–120. https://doi.org/10.1016/j.cej.2014.03.073

Zhao, G., Pang, B., Xu, Z., Peng, D., Xu, L., 2019. Assessment of urban flood susceptibility using semi-supervised machine learning model. Sci. Total Environ. 659, 940–949.

https://doi.org/10.1016/j.scitotenv.2018.12.217
Zhao, M., 2015. Research on least squares support vector machines algorithm, in: 2015 International Industrial Informatics and Computer Engineering Conference. Atlantis Press.
Zhou, P., Zhao, Y., Zhao, Z., Chai, T., 2015. Source mapping and determining of soil contamination by heavy metals using statistical analysis, artificial neural network, and adaptive genetic algorithm. J. Environ. Chem. Eng. 3, 2569–2579. https://doi.org/https://doi.org/10.1016/j.jece.2015.08.003
Zhou, Q.P., Jiang, H.Y., Wang, J.Z., Zhou, J.L., 2014. A hybrid model for $PM_{2.5}$ forecasting based on ensemble empirical mode decomposition and a general regression neural network. Sci. Total Environ. 496, 264–274. https://doi.org/10.1016/j.scitotenv.2014.07.051
Zhou, Y.L., Chang, F.J., Chang, L.C., Kao, I.F., Wang, Y.S., Kang, C.C., 2019. Multi-output support vector machine for regional multi-step-ahead $PM_{2.5}$ forecasting. Sci. Total Environ. 651, 230–240. https://doi.org/10.1016/j.scitotenv.2018.09.111
Zhu, J.J., Kang, L.L., Anderson, P.R., 2018. Predicting influent biochemical oxygen demand: Balancing energy demand and risk management. Water Res. 128, 304–313. https://doi.org/10.1016/j.watres.2017.10.053
Zhu, S.G., Han, H.G., Guo, M., Qiao, J.F., 2017. A data-derived soft-sensor method for monitoring effluent total phosphorus. Chinese J. Chem. Eng. 25, 1791–1797. https://doi.org/10.1016/j.cjche.2017.06.008
Zonouz, P.R., Niaei, A., Tarjomannejad, A., 2016. Modeling and optimization of toluene oxidation over perovskite-type nanocatalysts using a hybrid artificial neural network-genetic algorithm method. J. Taiwan Inst. Chem. Eng. 65, 276–285. https://doi.org/10.1016/j.jtice.2016.05.020